Original Research Article

Event-based lateral security control for network autonomous driving system subject to double-quantized scheme

Abstract

This paper investigates the event-based lateral security control problem for network autonomous driving system subject to the ideal path tracking performance, in which a novel double-quantized structure is reasonably integrated into a unified autonomous vehicle model. Firstly, a generalized tripled cyber-attack protocol, including deception attacks, DoS attacks and replay attacks is taken into consideration in this paper to simulate the interference of the external environment. Secondly, in order to improve the data transmission efficiency and relieve the effects of cyber-attacks, asynchronous even-triggered scheme (AETS) and doubled-quantized-based control protocol are introduced simultaneously. Additionally, with the help of elegant linearization technique, which not only makes the augmented closed-loop systems global exponential stability can be achieved, but also the desired output feedback controller gains and triggering parameter matrices are co-designed to ensure the H_∞ performance for the autonomous driving system. Finally, a practical example is given to verify the effectiveness of designed mentality.

Keywords: Autonomous vehicles; Multi-cyber-attacks; Networked control systems(NCSs); Quantization; Resilient event-triggered scheme

1. Introduction

With the high speed of development in recent years, the development of network control systems(NCSs) has also taken place in industry and other fields. It is characterized by the fact that the commands and responses of the control system are transmitted in a network as packets. Similarly, NCSs is becoming more and more widespread as more and more research is done in various application areas [1, 2].Also,due to the convenience of network communication and other advantages, NCSs exists in various fields. Such as space and land exploration, access to hazardous areas and related operations, plant automation, remote diagnostics and troubleshooting, experimental equipment, home robots, aircraft, vehicles, plant monitoring, security control of non-linear unmanned marine vehicle (UMV)[3] and hypersonic flight vehicles (HFVs)[4].Among them, vehicle steering control is the most common dynamic control. According to previous research,the advantages of automatic driving lie in reducing fatigue, improving comfort, optimizing fuel consumption and reducing pollution emissions [5, 6]. Therefore,path planning and control are particularly important for autonomous vehicles. How to take into account the comfort of the car in a safe situation is also a key issue. The difficulty with autonomous driving is the complexity of the road as the vehicle moves. How to make the vehicle work properly, the most common is to consider the lateral and vertical control of the vehicle in the case of obstacles. The current state of the car can be

clearly obtained by using the sensor and monitoring radar of the car, and images can be generated and uploaded for analysis of the surrounding perception. Then, the vehicle can be analyzed and the steering can be controlled by means of feedback control and other means. There have been several articles on vehicle control, such as PID control [7, 8], model predictive control [9, 10], fuzzy control [11, 31] and hybrid trigger control [12].

The fuzzy model proposed by Takagi and Sugeno has been improved by later generations and turned into today's dynamic model [13, 14], which has been widely used in many fields. Since T-S is an approximate model, some smooth nonlinear functions can be approximated with certain precision under convex sets. Under normal circumstances, Type-1 T-S cannot handle highly uncertain systems, whereas Type-2 T-S can.Compared with the dynamic system dealing with uncertainty, fuzzy Type-2 has more advantages [15–17]. It is a good choice to control vehicle lateral Angle in this paper [18]. At present, there are few such applications, generally some simple fuzzy models [18], which are not perfect in channel processing. In this paper, event triggering and quantization are adopted, and data in the channel is processed to further reduce the channel burden, so as to achieve accurate control of vehicles.Quantization is a good way to process data, which can save bandwidth resources by transforming real data into discrete form. At present, quantization [19, 32], dynamic quantization [33] and so on have been applied in various fields. On the quantization is one of the most common means of quantization, it can be on the boundary approximation method, this interference is with uncertainty. Generally, only the input of the controller is quantified [19, 34], but gradually, both the output and input of the control are quantified, resulting in a double quantization mechanism [20]. Combined with another way of saving bandwidth in this paper, they simultaneously process the data of the channel in the system, so as to make the whole system more smooth and save more bandwidth.As the most widely used and emerging communication scheme to reduce channel burden, research on ETS is maturing [21–23]. The feature of ETS is that only when its minimum rules are triggered, the next transmission will be carried out. In this way, Less useful data can be filtered out. At the same time, the threshold value can be used to adjust the channel transmission data according to the actual situation. Further, for the sensor to controller channels (S-C) and controller to actuator channels(C-A) to add asynchronous event triggering, the two channels respectively use threshold adjustment, which can not only reduce the burden of the channel, but also control the channel transmission respectively [24–26]. With the in-depth study of network control, network security has become an unavoidable problem after the processing of channel resources. Due to random attacks on the whole system, sensors are attacked [27], actuators are attacked [28], network channels [29] are attacked, and so on. And cyber-attacks are more likely to happen than any other. Network attacks are no longer a single attack. In practice, mixed attacks are often encountered, among which denial-of-service (DoS) attack and deception attack are the most common. deception attacks use data to replace real data to achieve the purpose of spoofing, while DoS attacks directly block data transmission. Considering the complexity of the actual situation, replay attack is introduced, which maliciously retransmits data, makes the channel burden greater, and may cause data omission and other problems [30]. Hybrid attack poses a great threat to the system.Considering the above situation, this paper adopts a new output feedback controller, which makes the whole system more easy to stabilize.To sum up, we adopts a new nonlinear autonomous driving lateral control system. In S-C and C-A channels, quantizers and event triggers are combined to reduce the burden of channels, while taking into account complex mixed attacks. The main contributions of this paper can be summarized as follows:

1. A generalized triple cyber-attack model is proposed,

including deception attacks, replay attacks, and DoS attacks. Meantime, the 2-freedom-degree-based fuzzy switching system is designed, in which combines with nonlinear, external disturbances, and multi-cyber-attacks to describe the effect of external complexities for the autonomous vehicle.

2. A novel double-quantized fuzzy output feedback controller is taken into consideration and some sufficient conditions is established to ensure the global exponential stability for the closed-loop system under AETS and doubled-quantized-based control protocol, for reducing non-conservative properties.
3. In conjunction with an example of the autonomous vehicleembedded in Carsim with Matlab, the lateral control of autonomous vehicle is analyzed with the help of the Carsim-Simulink to express the effectiveness and advantage of the controller.

The structure of this article is as follows. In the section II, the vehicle dynamics model, quantizer, event triggering scheme, hybrid attack and closed-loop system are presented. The main results are given in section III. In the section IV, combined with Carsim and Matlab, the actual examples in this paper are used for simulation experiments. Finally, the conclusion is presented in the section V.

2. System Modeling And Problem Formulation

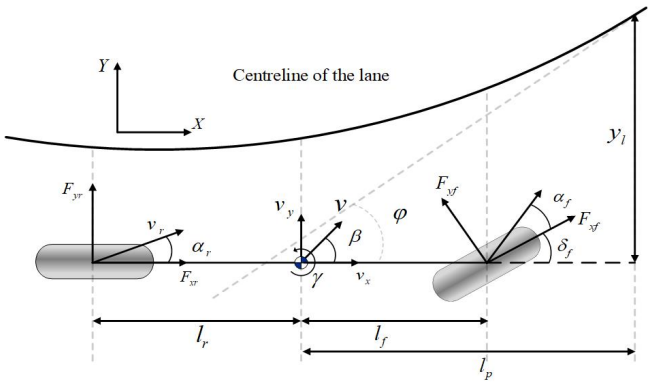

Figure 1: Caption

In this paper, the vehicle dynamic model is adopted, which shows strong nonlinear condition. The output feedback controller of the vehicle is designed according to this condition. Fig. 1 shows a widely used vehicle dynamic model for steering analysis and fuzzy system design.

Before presenting the model, we present the parameters of the cart as shown in the following table:

Table 1: Dynamic model of single-track vehicle

Symbols	Descriptions
m	vehicle mass (kg)
f, r	subscripts denoting front and rear
J_z	vehicle yaw moment of inertia $(\mathrm{kg}\cdot\mathrm{m}^2)$
l_p	preview distance (m)
$l_{f,r}$	distance of center of gravity from front/rear axle (m)
$C_{\alpha i}$	cornering stiffness (N/rad)
$\mathfrak{F}_{xi}$	longitudinal tire/road forces (N), $i = f, r$
$\mathfrak{F}_{yi}$	lateral tire/road forces (N), $i = f, r$
y_l	lateral offset from the road centerline at a preview distance (m)
φ	relative yaw angle (rad)
δ_f	front wheel steering angle (rad)
γ	vehicle yaw rate (rad/s)
$\alpha_{f,r}$	front/rear tire slip angle (rad)
β	vehicle side slip angle (rad)
v_x, v_y	vehicle longitudinal and lateral speeds (m/s)
$\varkappa$	road curvature
d	radius of road curves (m)

2.1. Vehicle Modeling

Having summarised Fig. 1 and Table 1 above. Considering the dynamics to which a wheel is subjected, the longitudinal force F_{xr} can be neglected in the overall system. The dynamics of the vehicle is therefore described by the following equations:

$$\begin{aligned} m\left(\dot{v}_x - \gamma v_y\right) &= \mathfrak{F}_{xf}\cos\delta_f - \mathfrak{F}_{yf}\sin\delta_f \\ m\left(\dot{v}_y + \gamma v_x\right) &= \mathfrak{F}_{xf}\sin\delta_f + \mathfrak{F}_{yf}\cos\delta_f + \mathfrak{F}_{yr} \\ J_z\dot{\gamma} &= l_f\left(\mathfrak{F}_{xf}\sin\delta_f + \mathfrak{F}_{yf}\cos\delta_f\right) - l_r\mathfrak{F}_{yr} \end{aligned} \tag{1}$$

Then we consider replacing the equation $v_y = v_x\tan\beta$ with the dynamic cart model inequality, which is then expressed as follows:

$$\begin{aligned} \mathfrak{F}_{yf} + \mathfrak{F}_{yr} &= mv_x(\dot{\beta} + \gamma) \\ l_{f\mathfrak{F}_y} - l_r\mathfrak{F}_{yr} &= J_z\dot{\gamma} \end{aligned} \tag{2}$$

Since tyre sliding is of small magnitude, then $\mathfrak{F}_{yf}$ and $\mathfrak{F}_{yr}$ can be defined approximately as:

$$\begin{aligned} \mathfrak{F}_{yf} &= -2C_\alpha\alpha_f, \alpha_f \approx \beta + \frac{\gamma_f}{v_x} - \delta_f \\ \mathfrak{F}_{yr} &= -2C_{\alpha r}\alpha_r, \alpha_r \approx \beta - \frac{rl_r}{v_x} \end{aligned} \tag{3}$$

In the actual process, due to the complexity of the road, there may be an offset in the variables, which we do not consider here. For the path-tracking problem in autonomous driving, based on the above, the offset distance y_l can be derived with respect to the vehicle's forward direction and the offset angle of the road tangent l_p used to represent the dynamic condition of the vehicle. The error model of the vehicle dynamics is then represented as follows:

$$\begin{aligned} \dot{y}_l &= \beta_{v_x} + l_p\gamma + v_x\varphi \\ \dot{\varphi} &= \gamma - \varkappa v_x \end{aligned} \tag{4}$$

Combining equations (2)-(4), we can obtain a dynamic model of vehicle

$$\dot{x}(t) = Ax(t) + Bu(t) + B_\omega\omega(t) \tag{5}$$

where $x(t) = \begin{bmatrix} \beta & \gamma & \varphi_e & y_l \end{bmatrix}^T$, $x(t) \in \mathbb{R}^{n_x}, u(t) = \sigma_f$, and $\omega(t) = \kappa = (1/R)$ with R the curvature radium and

$$A = \begin{bmatrix} \frac{-2C_{\alpha f}-2C_{\alpha r}}{mv_x} & \frac{-2l_fC_{\alpha f}+2l_rC_{\alpha r}}{mv_x^2} - 1 & 0 & 0 \\ \frac{-2l_fC_{\alpha f}+2l_rC_{\alpha r}}{I_z} & \frac{-2l_f^2C_{\alpha f}-2l_r^2C_{\alpha r}}{I_zv_x} & 0 & 0 \\ 0 & 1 & 0 & 0 \\ v_x & l_p & v_x & 0 \end{bmatrix}$$

$$B = \begin{bmatrix} \frac{2C_{\alpha f}}{mv_x} \\ \frac{2l_fC_{\alpha f}}{I_z} \\ 0 \\ 0 \end{bmatrix}, B_\omega = \begin{bmatrix} 0 \\ 0 \\ -v_x \\ 0 \end{bmatrix}.$$

Remark 1:For the simplified version of the autonomous vehicle model, it can be concluded that the γ can get data from the navigation installed in the self-driving vehicle. v_x can be measured using an odometer. φ_e can be measured using an optical encoder in the car. y_l and φ_e can be obtained from the camera. At the same time, v_y and β be can be measured by the dual-antenna GPS system or the Corevit optical sensors.For resource-saving purposes, we can just take γ, φ_e and y_l as input. Similarly, for the control design, the performance output includes vehicle direction deviation, driver comfort and passenger comfort requirements, which we can take $z(t) = \begin{bmatrix} \varphi_e, & y_l, & a_y \end{bmatrix}^T$,where $a_y = v_x\gamma$.

2.2. Vehicle Dynamic Of Fuzzy Model

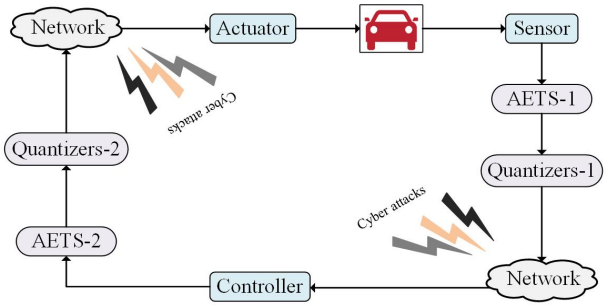

Figure 2: The networked vehicle system.

Fig. 2 depicts a schematic diagram of a quantization and event-triggered fuzzy system based on hybrid network attacks

In practice, the speed of the vehicle will be limited, so we set $\underline{v} \leq v_x(t) \leq \bar{v}$, where $\underline{v}$ and $\bar{v}$ represent the maximum and minimum values. Based on the above analysis of lateral vehicles, the following T-S fuzzy model can be obtained

Rule i : If $\mathfrak{g}_1(t)$ is $\mathcal{G}_1^i, \mathfrak{g}_2(t)$ is $\mathcal{G}_2^i$, and $\mathfrak{g}_3(t)$ is $\mathcal{G}_3^i$,then

$$\begin{cases} \dot{x}(t) = A_ix(t) + B_{1i}u(t) + B_{2i}\omega(t) \\ y(t) = Cx(t) \\ z(t) = D_ix(t), i = 1, 2, \ldots, r \end{cases} \tag{6}$$

where $\mathfrak{g}_1(t) = v_x(t), \mathfrak{g}_2(t) = \frac{1}{v_x(t)}$, and $\mathfrak{g}_3(t) = \frac{1}{v_x^2(t)}$ are premise variables; $\mathcal{G}_j^i$ is the fuzzy sets of fuzzy rule

i with $j = 1, 2, 3$ corresponding to the premise variables $\mathfrak{g}_1(t), \mathfrak{g}_2(t)$, and $\mathfrak{g}_3(t)$; and A_i, B_{1i}, B_{2i}, and D_i are system matrices which are defined by (5) with $v_x(t)$ being replaced by $\underline{v}$ and $\bar{v}$, respectively.

According to (6), the global lateral vehicle dynamics fuzzy model can be rewritten as the following

$$\begin{cases} \dot{x}(t) = \sum_{i=1}^{2} \chi_i(\mathfrak{I}_g(t))(A_i x(t) + B_{1i}u(t) + B_{2i}\omega(t)) \\ y(t) = Cx(t) \\ z(t) = \sum_{i=1}^{2} \chi_i\left(\mathfrak{I}_g(t)\right) D_i x(t) \end{cases} \tag{7}$$

witch are satisfying $\sum_{i=1}^{r} \chi_i(g(t)) = 1$. Based on Taylor's approximation, $\mathfrak{g}_1(t), \mathfrak{g}_2(t)$ and $\mathfrak{g}_3(t)$ can be written as follows:

$$\begin{aligned} \mathfrak{g}_2(t) &= \frac{1}{v_x(t)} = \frac{1}{v_0} + \frac{1}{v_1}\mathfrak{I}_g(t) \\ \mathfrak{g}_1(t) &= v_x(t) \cong v_0\left(1 - \frac{v_0}{v_1}\mathfrak{I}_g(t)\right) \\ \mathfrak{g}_3(t) &= \frac{1}{v_x^2(t)} \cong \frac{1}{v_0^2}\left(1 + 2\frac{v_0}{v_1}\mathfrak{I}_g(t)\right) \end{aligned}$$

where $-1 \leq \mathfrak{I}_g(t) \leq 1$ is used to describe the changes of $v_x(t)$ between the bounds $\underline{v}$ and $\bar{v}$, and we have

$$v_0 = \frac{2\underline{v}\bar{v}}{\underline{v} + \bar{v}}, v_1 = \frac{2\underline{v}\bar{v}}{\underline{v} - \bar{v}}$$

2.3. Resilient Event-Triggered Schemes

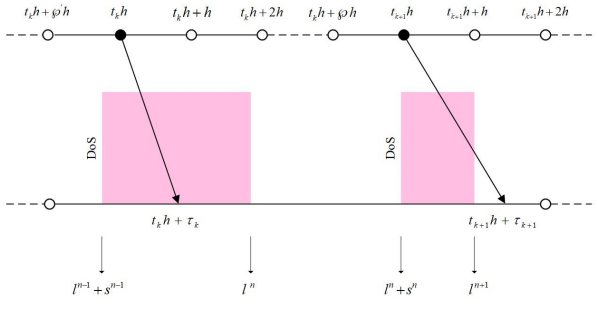

Figure 3: Example of event trigger evolution and DoS attack blocking data

Fig. 3 shows an example of an event-trigger sampling and release instants under the DoS attacks. For the event-trigger part, $t_k h$ and $t_g h$ are the triggering instant of the sensor and controller, and the entry event is triggered. $h > 0$ is the sampling period.When attacks are absent, the next transmission instant of AETS-1 and AETS-2 can be defined as

$$\begin{aligned} t_{k+1}h = t_k h + \inf_{p\geq 1}\{ph|(Ce_s(t))^T\Omega_s Ce_s(t) \\ - \sigma_s y^T(t_k h)\Omega_s y(t_k h) \geq 0\} \\ t_{g+1}h = t_g h + \inf_{q\geq 1}\{qh|(e_c(t))^T\Omega_c e_c(t) \\ - \sigma_c x_c^T(t_g h)\Omega_c x_c(t_g h) \geq 0\} \end{aligned} \tag{8}$$

where p, q=1,2,3,..., σ_s and σ_c indicate constant thresholds belong to (0,1]. Ω_s and Ω_c are the weight of triggering condition which need to be designed.

For S-C channels, $t \in [t_k h + \tau_k, t_{k+1} + \tau_{k+1})$. Define $\tau_s(t) = t - t_k h$. We need to consider the following two case

Case 1 : Suppose that $t_k h + h + \bar{\tau} > \tau_{k+1}$, where $\tau \leqslant \bar{\tau} < h$, then

$$\tau_k \leqslant \tau_s(t) \leqslant t_{k+1}h + \tau_{k+1} - t_k h \leqslant h + \bar{\tau} \tag{9}$$

Case 2 : Suppose that $t_k h + h + \bar{\tau} < t_{k+1}h + \tau_{k+1}$. Then it can be divided into two time intervals, respectively $[t_k h + \tau_k, t_k h + h + \bar{\tau})$ and $[t_k h + ph + \bar{\tau}.t_k h + (p+1)h + \bar{\tau})$. We can get when there exists a positive integer $\wp$

$$t_k h + \wp h + \bar{\tau} < t_{k+1}h + \tau_{k+1} \leqslant t_k h + (\wp + 1)h + \bar{\tau} \tag{10}$$

Then we can divide $[t_k h + \tau_k, t_{k+1} + \tau_{k+1})$ as follow:

$$[t_k h + \tau_k, t_{k+1} + \tau_{k+1}) = \mho_0 \cup \bigcup_{p=1}^{\wp-1} \mho_p \cup \mho_\wp \tag{11}$$

where

$$\mho_0 = [t_k h + \tau_k, t_k h + h + \bar{\tau}),$$

$$\mho_p = [t_k h + \bar{\tau} + ph, t_k h + \bar{\tau} + (p+1)h), p = 1, 2, ...\wp,$$

$$\mho_\wp = [t_k h + \bar{\tau} + \wp h, t_{k+1}h + \tau_{k+1})$$

So we can define

$$\tau_s(t) = \begin{cases} t - t_k h, & t \in \mho_0 \\ t - t_k h - ph, & t \in \mho_p, p = 1, 2, ..., \wp - 1 \\ t - t_k h - \wp h, & t \in \mho_\wp \end{cases} \tag{12}$$

Then the error is

$$e_s(t) = \begin{cases} 0, & t \in \mho_0 \\ y(t_k h) - y(t_k h + ph), & t \in \mho_p \\ y(t_k h) - y(t_k h + \wp h), & t \in \mho_\wp \end{cases} \tag{13}$$

And the same thing happens for the C-A channel. Therefore for$t \in [t_k h + \tau_k, t_{k+1} + \tau_{k+1})$, the AETS between the current trigger data and the sampled data is also defined as follows

$$\begin{aligned} (Ce_s(t))^T \Omega_s Ce_s(t) < \sigma_s y^T(t_k h)\Omega_s y(t_k h) \\ (e_c(t))^T \Omega_c e_c(t) < \sigma_c x_c^T(t_g h)\Omega_c x_c(t_g h) \end{aligned} \tag{14}$$

where

$$\begin{aligned} Ce_s(t) = y(t_k h) - y(t_k h - \tau_s(t)) \\ e_c(t) = x_c(t_g h) - x_c(t_g h - \tau_c(t)) \end{aligned}$$

2.4. Double Quantization

The signals transmitted from the sensor and controller respectively enter the quantizers through the event triggering mechanism. Here, logarithmic quantizers are used to process the data. Then given a vector $\ell = [\ell_1 \quad \ell_2 ... \quad \ell_n]^T$. Here ℓ is the outgoing data by the event triggered. The $f(\cdot)$ is adapted as $f(\ell) = [f_1(\ell_1) \quad f_2(\ell_2) \cdots \quad dotf_n(\ell_n)]^T$. So we can define for logarithmic $f_\imath(\ell_\imath)(\imath = 1, 2, ..., n)$ as

$$f_\imath(\ell_\imath) = \begin{cases} u_\mathfrak{r}^\imath, & if \frac{u_\mathfrak{r}^\imath}{1+\iota_{f_\imath}} \leqslant \ell_\imath \leqslant \frac{u_\mathfrak{r}^\imath}{1-\iota_{f_\imath}}, \ell_\imath > 0 \\ 0, & if \ell_\imath = 0 \\ -f_\imath(\ell_\imath), & if \ell_\imath < 0 \end{cases} \tag{15}$$

where $\iota_{f_\imath} = (1 - \rho_{f_\imath})/(1 + \rho_{f_\imath})$, and the quantization density is a constant for $0 < \rho_{f_\imath} < 1$, $u_\mathfrak{r}^\imath \in \mathfrak{U}_\imath$ is the quantization level, $\mathfrak{U}_\imath = \left\{ \pm u_\mathfrak{r}^\imath : u_\mathfrak{r}^\imath = \rho_{f_\imath}^\mathfrak{r} u_0^\imath, \mathfrak{r} = \pm 1, \pm 2, ... \right\} \cup \{\pm u_0^\imath\} \cup$
$\{0\}$ with $u_0^\imath > 0$.

Then we define $\Delta_f = diag\{\Delta_{f_1}, \Delta_{f_2}, ..., \Delta_{f_n}\}, \Delta_{f_\ell} \in [-\iota_{f_\imath}, \iota_{f_\imath}], \ell = 1, 2, ..., n$. Then the data from the sensor and processed by the quantizers can be obtained as follows

$$f(\ell) = (I + \Delta_f)\ell \tag{16}$$

This is the quantization of the S-C channel, and the corresponding, in the C-A channel, we define $g(\ell) = [g_1(\ell_1)$ $g_2(\ell_2) \cdots g_n(\ell_n)]^T$. In the same way,for $\ell = 1, 2, ..., n$, through (14) we have

$$g(\ell) = (I + \Delta_g)\ell \tag{17}$$

where $\Delta_g = diag\{\Delta_{g_1}, \Delta_{g_2}, ..., \Delta_{g_n}\}$,$\Delta_{g_\ell} \in [-\iota_{g_\imath}, \iota_{g_\imath}]$ $\iota_{g_\imath} = (1 - \rho_{g_\imath})/(1 + \rho_{g_\imath})$,$\rho_{g_\imath}$ also is the quatization density of $g_\imath(\cdot)$

For this paper, the data is quantized after event triggering and then entering the quantizer. So ℓ represents the data after the event triggered, respectively $y(t_k h)$ and $u_c(t_g h)$. Then, by combining equations (14)-(16), the following results can be obtained

$$\begin{aligned} f(y(t_k h)) = (I + \Delta_f)y(t_k h) \\ f(u_c(t_g h)) = (I + \Delta_g)u_c(t_g h) \end{aligned} \tag{18}$$

where $y(t_k h)$ and $u_c(t_g h)$ are the output signals of the sensor and controller.

2.5. Multi-cyber-attacks

It can also be seen from Fig. 2 that there are three attack modes, which occur in two channels, for the S-C and C-A channels. After the data is processed by the logarithmic quantizers, it will encounter deception attack first. To reflect the randomness of the attack, we set the Bernoulli variable $\alpha_s(t)$ and $\alpha_c(t)$. These two variables satisfy

$$\begin{aligned} E\{\alpha_s(t)\} = \bar{\alpha}_s, E\left\{(\alpha_s(t) - \bar{\alpha}_s)^2\right\} = \theta_{s1}^2 \\ E\{\alpha_c(t)\} = \bar{\alpha}_c, E\left\{(\alpha_c(t) - \bar{\alpha}_c)^2\right\} = \theta_{c1}^2 \end{aligned}$$

where $\bar{\alpha}_s$ and $\bar{\alpha}_c$ are non-negative given constants. Therefore, in network transmission, after deception attacks, data will be replaced by

$$\begin{aligned} y_1(t) &= (1-\alpha_s(t))F_s(t) + \alpha_s(t)f(y(t_k h)) \\ u_1(t) &= (1-\alpha_c(t))F_c(t) + \alpha_c(t)f(x_c(t_g h)) \end{aligned} \tag{19}$$

where $F_c(t)$ and $F_s(t)$ as the deception attacks in the S-C and C-A channnels.

Then, immediately after that, the second attack is the replay attack. When attacks occurs, the original data starts back up. Again, for uncertainty, Bernoulli variables $\beta_s(t)$ and $\beta_s(t)$. Again, satisfaying

$$\begin{aligned} E\{\beta_s(t)\} = \bar{\beta}_s, E\left\{(\beta_s(t)-\bar{\beta}_s)^2\right\} = \theta_{s2}^2 \\ E\{\beta_c(t)\} = \bar{\beta}_c, E\left\{(\beta_c(t)-\bar{\beta}_c)^2\right\} = \theta_{c2}^2 \end{aligned}$$

If the data is in the channel and is under replay attack, it can be written as

$$\begin{aligned} y_2(t) &= (1-\beta_s(t))y_m(t) + \beta_s(t)y_1(t) \\ u_2(t) &= (1-\beta_c(t))u_n(t) + \beta_c(t)u_1(t) \end{aligned} \tag{20}$$

where $y_m(t)$ and $u_n(t)$ indicate the replay signal.The time of the replay attack is unknown, after this attack occurs, replay back before the event triggered.At the same time, since the attack time of the attacker is generally fixed and relatively small, both $m(t)$ and $n(t)$ have upper limits.Then we set to $0 < m(t) < m_M$ and $0 < n(t) < n_M$.

Remark 2:For replay attacks, after the attack is triggered, the data goes back to before the event was triggered. At the same time, after the delay $m(t)$ and $n(t)$ of the replay attack, an event-triggered delay $\tau(t)$ needs to be experienced again. Here, for convenience, it is assumed that the delay triggered by the event is much smaller than that of the replay attack, so there are only $t-m(t)$ and $t-n(t)$ in the formula.

The third and final attack is a DoS attack.As we can see in figure 3,this attack does not modify the data signal to continue down the transmission, but instead when an attack occurs, no signal can be transmitted to the next section; When the DoS attack dormant period, the signal can remain unchanged and continue to transmit. Because of the above characteristics, then the DoS attack transmission data can be written as

$$\begin{aligned} y_3(t) &= \begin{cases} y_2(t), & t \in \mathcal{L}_1^n \\ 0, & t \in \mathcal{L}_2^n \end{cases} \\ u_3(t) &= \begin{cases} u_2(t), & t \in \mathcal{L}_1^n \\ 0, & t \in \mathcal{L}_2^n \end{cases} \end{aligned} \tag{21}$$

where $\mathcal{L}^n = \mathcal{L}_1^n + \mathcal{L}_2^n$,$\mathcal{L}^n$ indicates that the DoS attack occurred for the $(n+1)$ time,and $n \in \mathcal{N}$ indicates each time period during which the attack occurs.It can be clearly seen that, when there is no attack, is $\mathcal{L}_1^n = [\mathfrak{l}^n, \mathfrak{D}^n)$;in contrast, when an attack occurs, no data is transmitted, then $\mathcal{L}_2^n = \left[\mathfrak{D}^n, \mathfrak{l}^{n+1}\right)$,where $\mathfrak{D}^n = \mathfrak{l}^n + \mathfrak{s}^n$.$\mathfrak{l}^n$ and $\mathfrak{s}^n$ indicate the start and start of sleep of the $(n+1)th$ DoS attack, respectively.Therefore, it can be concluded that the DoS attack satisfy $0 = \mathfrak{l}^0 < \mathfrak{s}^0 < \mathfrak{l}^1 < \mathfrak{D}^1 < \mathfrak{l}^2 < \cdots < \mathfrak{D}^n < \mathfrak{l}^{n+1}$.

Assumption 1:Because of the particularity of attacks, the dormant and active periods of DoS attacks must meet a finite time.

$$\begin{cases} s_{min} \leq \inf_{n\in N}\{\mathfrak{s}^n\} \\ d_{max} \geq \sup_{n\in N}\left\{\mathfrak{l}^{n+1} - (\mathfrak{D}^n)\right\} \end{cases}$$

Assumption 2:For $n(0,t) = card\{n \in N | t > \mathfrak{D}^n\}$ represents the transition between the dormant and active phases of DoS attacks in $[0,t)$, and card represents the number of elements.So there is $\hbar_1 \geq 0$ and $\hbar_2 > h$, and for all t, the DoS attack is satisfied $n(0,t) \leq \hbar_1 + (t/\hbar_2)$

By combining all the mixed attacks (18), (20) and (21), the final attack formula can be obtained as follows

$$\breve{y}(t)=\begin{cases}(1-\beta_s(t))y_m(t)+((1-\alpha_s(t))\beta_s(t)F_s(t)\\+(I+\Delta_f)\alpha_s(t)\beta_s(t)y(t_kh),t\in\mathcal{L}_1^n\\0,t\in\mathcal{L}_2^n\end{cases}$$

$$u(t)=\begin{cases}(1-\beta_c(t))u_n(t)+(1-\alpha_c(t))\beta_c(t)F_c(t)\\+(I+\Delta_g)\alpha_c(t)\beta_c(t)u_c(t_gh),t\in\mathcal{L}_1^n\\0,t\in\mathcal{L}_1^n\end{cases}\tag{22}$$

Remark 3:The three attacks in this paper all meet certain bounded conditions. In reality, if the attack time exceeds a certain period, the system may break down directly.At the same time, we can find that the attack sequence of this paper follows the deception attack first, then the replay attack, and finally the DoS attack, but in reality, the attacks are random and uncertain. If random, then two channels, a total of three attacks, too many combination ways, too complicated discussion, this is not the main discussion of this paper, so simplify the order.Of course, in the actual process, the attack sequence can be detected, which is basically the same as the steps in the above sequence.

2.6. Output-Feedback Controller

The output feedback control rules based on lateral vehicles are as follows

Rule j:If $h_1(t)$ is $\mathfrak{H}_1^j$, $h_2(t)$ is $\mathfrak{H}_2^j$, and $h_3(t)$ is $\mathfrak{H}_3^j$, then

$$\begin{cases}\dot{x}_c(t)=A_j^cx_c(t)+L_j^c\breve{y}(t)\\u_c(t)=C_j^cx_c(t)\end{cases}\tag{23}$$

where A_j^c,L_j^c,and $C_j^c$are the control gains to be designed,and $x_c(t)$ is the state of the output-feedback controller. For the sake of follow equation, we define $F_s(t)=Cf_s(y(t_kh))$ and $F_c(t)=C_j^cf_c(x_c(t_gh))$. The global controller can be written as

$$\begin{cases}\dot{x}_c(t)=\sum_{j=1}^{2}\chi_j(\mathfrak{I}_h(t_kh))[A_j^cx_c(t)+L_j^c\breve{y}(t)]\\u_c(t)=\sum_{j=1}^{2}\chi_j(\mathfrak{I}_h(t_kh))C_j^cx_c(t)\end{cases}\tag{24}$$

Assumption 3:For spoofing attacks, we have $f_s(y(t_kh))$ and $f_c(x_c(t_gh))$ unknown but elastic, then for the real constant matrix $\mathcal{F}_s$ and $\mathcal{F}_c$, they satisfying

$$\begin{aligned}\|f_s(y(t_kh))\|_2\le\|\mathcal{F}_sy(t_kh)\|_2\\\|f_c(x_c(t_gh))\|_2\le\|\mathcal{F}_cx_c(t_gh)\|_2\end{aligned}\tag{25}$$

Remark 4:Since this paper uses two channels for processing, $\breve{y}(t)$ and $u_c(t)$ are both signals entering the processing, $\breve{y}(t)$ enters the S-C channel and $u_c(t)$ enters the C-A channel. Ii need to be careful when dealing with it.

2.7. System Formulation

By combining the system, the event trigger 13, the quantization 17, the hybrid attack 21, and the controller 23, we have the following results, namely the vehicle dynamic output-feedback system.

$$\dot{\eta}(t)=\begin{cases}\sum_{i=1}^{2}\sum_{j=1}^{2}\chi_i\chi_j[\mathbb{A}_{ij}^1\eta(t)+(I-\bar{\beta}(t))\mathbb{B}_{ij}^o\eta(t-o(t))+\\(I-\bar{\beta}(t))\mathbb{B}_{ij}^{oe}e(t-o(t))+(I-\bar{\alpha}(t))\bar{\beta}(t)\mathbb{B}_{ij}^ff(t)\\+\bar{\alpha}(t)\bar{\beta}(t)\mathbb{B}_{ij}^\tau\eta(t-\tau(t))+\bar{\alpha}(t)\bar{\beta}(t)\mathbb{B}_{ij}^ee(t)+\\\mathbb{B}_{\omega i}\omega(t)],t\in\mathcal{L}_1^n\\\sum_{i=1}^{2}\sum_{j=1}^{2}\chi_i\chi_j[\mathbb{A}_{ij}^2\eta(t)+\mathbb{B}_{\omega i}\omega(t)],t\in\mathcal{L}_2^n\end{cases}\tag{26}$$

$$z(t)=\sum_{i=1}^{2}\chi_iD_iH_1\eta(t)$$

where χ_i and χ_j stand for $\chi_i(\mathfrak{I}_g(t))$ and $\chi_j(\mathfrak{I}_h(t_kh))$, respecltively, and

$$\eta(t)=\begin{bmatrix} x(t) \\ x_c(t) \end{bmatrix}, \eta(t-o(t))=\begin{bmatrix} x(t-m(t)) \\ x_c(t-n(t)) \end{bmatrix},$$
$$\eta(t-\tau(t))=\begin{bmatrix} x(t_hk-\tau_s(t)) \\ x_c(t_gh-\tau_c(t)) \end{bmatrix}, f(t)=\begin{bmatrix} f_s(x(t_kh)) \\ f_c(x_c(t_gh)) \end{bmatrix},$$
$$e(t-o(t))=\begin{bmatrix} e_s(t-m(t)) \\ e_c(t-n(t)) \end{bmatrix}, e(t)=\begin{bmatrix} e_s(t) \\ e_c(t) \end{bmatrix},$$
$$\bar{\alpha}(t)=\begin{bmatrix} \alpha_c(t) & 0 \\ 0 & \alpha_s(t) \end{bmatrix}, \bar{\beta}(t)=\begin{bmatrix} \beta_c(t) & 0 \\ 0 & \beta_s(t) \end{bmatrix},$$
$$\mathbb{A}_{ij}^1=\begin{bmatrix} A_i & 0 \\ 0 & A_j^{c1} \end{bmatrix}, \mathbb{A}_{ij}^2=\begin{bmatrix} A_i & 0 \\ 0 & A_j^{c2} \end{bmatrix},$$
$$\mathbb{B}_{ij}^o=\begin{bmatrix} 0 & B_{1i}C_j^c \\ L_j^cC & 0 \end{bmatrix}, \mathbb{B}_{ij}^o=\mathbb{B}_{ij}^{oe}=\mathbb{B}_{ij}^f,$$
$$\mathbb{B}_{ij}^\tau=\begin{bmatrix} 0 & (I+\Delta_g)B_1iC_j^c \\ (I+\Delta_f)L_j^cC & 0 \end{bmatrix}, \mathbb{B}_{ij}^\tau=\mathbb{B}_{ij}^e,$$
$$\mathbb{B}_{\omega i}=\begin{bmatrix} B_{2i} \\ 0 \end{bmatrix}, H_1=[I_{nx}, 0_{nx}]$$

This paper mainly designs the dynamic output-feedback controller. If stability is needed, it needs to meet the following requirements.

1. The system in (25) is exponential stable.
2. Under zero intial condition,$\gamma>0$ is a given positive scalar.$\|z(t)\|_2 \leq \gamma \|\omega(t)\|$ holds for any nonzero $\omega(t)$

lemma 1:For given x, y,and a free martrix $\mathbb{U}$,the following inequality holds:

$$-2x^Ty \leq x^T\mathbb{U}^{-1}x+y^T\mathbb{U}y$$

lemma 2:For the given positive-definite matrices R,P and scalar $\mathfrak{e}$,the following holds:

$$-PR^-1P \leq -2\mathfrak{e}P+\mathfrak{e}^2R \tag{27}$$

3. Main Results

In this section, we first demonstrate the stability of the system after event-triggered, quantified, and hybrid attacks, and then we need to design the controller. So the main results are as follows

Theorem 1:For given positive scalars $\tau_M, o_M, \bar{\alpha}_s, \bar{\alpha}_c, \bar{\beta}_s, \bar{\beta}_c, \theta_{s1}, \theta_{c1}, \theta_{s2}, \theta_{c2}, \partial_\delta(\delta=1,2)$is the hybrid attack probability,the limitations of DoS attack s_{min}, d_{max},samping period h.System (27) is globally exponential stable with H_∞ level $\breve{\gamma}$.If there exist positive matrices $\Omega_s, \Omega_c, P_1, P_2, Q_{11}, Q_{12}, Q_{21}, Q_{22}, R_{11}, R_{12}, R_{21}$,and R_{22}, $A_j^{c\delta}, C_j^c, L_j^c$ to satisfy the controller and free matrices $M_\delta, J_\delta, N_\delta, K_\delta, \chi_j-\kappa_j\beth_j>0$,$0<\kappa_j\leq 1$ satisfying the following:

$$\Theta_\delta<0 \tag{28}$$

$$\Theta_{ij}^\delta+\Theta_{ji}^\delta-\mathfrak{S}_i^\delta-\mathfrak{S}_j^\delta<0 \tag{29}$$

$$\kappa_j\Theta_{ij}^\delta+\kappa_i\Theta_{ji}^\delta-\kappa_j\mathfrak{S}_i^\delta-\kappa_i\mathfrak{S}_j^\delta+\mathfrak{S}_i^\delta+\mathfrak{S}_j^\delta<0 \tag{30}$$

$$P_1\leq\partial_2P_2 \tag{31}$$

$$P_2\leq\partial_1e^{2(\vartheta_1+\vartheta_2)}P_1 \tag{32}$$

$$Q_\delta\leq\partial_{3-\delta}Q_{3-\delta} \tag{33}$$

$$R_\delta\leq\partial_{3-\delta}R_{3-\delta} \tag{34}$$

where

$$\Theta_{ij}^\delta=\Theta_\delta+z^T(t)z(t)-\breve{\gamma}^2\omega^T(t)\omega(t)$$
$$\Theta_1=\begin{bmatrix} \Xi_{11} & \Xi_{12} & \Xi_{13} & \Xi_{14} \\ * & \Xi_{16} & 0 & 0 \\ * & * & \Xi_{17} & 0 \\ * & * & * & \Xi_{18} \end{bmatrix}$$
$$\Xi_{11}=\Phi_1+\jmath_1\Pi_1^T+\jmath_1\Pi_1, \Xi_{16}=diag\{I,I\}$$

$$\Xi_{12}=\begin{bmatrix} 0 & 0 & 0 & \pounds_{10}^T & 0 & 0 & \pounds_{11}^T & 0 & 0 \end{bmatrix}^T$$

$$\Xi_{13}=\begin{bmatrix}\pounds_{12}^T & \pounds_{13}^T & 0 & \pounds_{14}^T & 0 & \pounds_{15}^T \\ & & & \pounds_{16}^T & \pounds_{17}^T & \pounds_{18}^T\end{bmatrix}^T$$

$$\Xi_{17}=diag\left\{-P_1R_1^{-1}P_1,-P_1R_1^{-1}P_1,\right.$$
$$\left.-P_1R_1^{-1}P_1,-P_1R_1^{-1}P_1\right\}$$

$$\Xi_{18}=diag\left\{-\jmath_1R_{11},-\jmath_1R_{11},-\jmath_1R_{12},-\jmath_1R_{12}\right\}$$

$$\Phi_1=\begin{bmatrix}\pounds_1 & \pounds_2 & \pounds_3 & \pounds_4 & \pounds_5\\ * & \pounds_6 & 0 & 0 & 0\\ * & * & \pounds_7 & 0 & 0\\ * & * & * & 0 & 0\\ * & * & * & * & \pounds_9\end{bmatrix}$$

$$\pounds_1=2\zeta_1P_1+sym\left\{P_1\mathbb{A}_{ij}^1\right\}+Q_{11}+Q_{12}$$

$$\pounds_2=\begin{bmatrix}(I-\bar{\beta})P_1\mathbb{B}_{ij}^o & 0 & \bar{\alpha}\bar{\beta}P_1\mathbb{B}_{ij}^\tau & 0\end{bmatrix}$$

$$\pounds_3=\begin{bmatrix}(I-\bar{\beta})P_1\mathbb{B}_{ij}^{oe} & \bar{\alpha}\bar{\beta}P_1\mathbb{B}_{ij}^e\end{bmatrix}$$

$$\pounds_4=P_1\mathbb{B}_{\omega i},\pounds_5=(I-\bar{\alpha})\bar{\beta}P_1\mathbb{B}_{ij}^f$$

$$\pounds_6=diag\left\{\sigma_sH_1^TC^T\Omega_sCH_1+\sigma_cH_2^T\Omega_cH_2,-\jmath_1Q_{12},\right.$$
$$\left.\sigma_sH_1^TC^T\Omega_sCH_1+\sigma_cH_2^T\Omega_cH_2,-\jmath_1Q_{11}\right\}$$

$$\pounds_7=diag\left\{(\sigma_s-1)H_1^TC^T\Omega_sCH_1+(\sigma_c-1)H_2^T\Omega_cH_2,\right.$$
$$\left.(\sigma_s-1)H_1^TC^T\Omega_sCH_1+(\sigma_c-1)H_2^T\Omega_cH_2\right\}$$

$$\pounds_9=diag\left\{-H_1^TH_1-H_2^TH_2\right\}$$

$$\pounds_{11}=[F_s^TC^TH_1^T\quad F_c^TH_2^T],\pounds_{11}=\pounds_{10}$$

$$\pounds_{12}=[\mathbb{A}_{ij}^{1T}P_1\quad 0\quad 0\quad 0]$$

$$\pounds_{13}=[(I-\bar{\beta})\mathbb{B}_{ij}^{oT}P_1\quad -\theta_2\mathbb{B}_{ij}^{oT}P_1]$$

$$\pounds_{14}=\begin{bmatrix}\bar{\alpha}\bar{\beta}\mathbb{B}_{ij}^{\tau T}P_1 & \theta_2\bar{\alpha}\mathbb{B}_{ij}^{\tau T}P_1 & \theta_1\bar{\beta}\mathbb{B}_{ij}^{\tau T}P_1 & \theta_1\theta_2\mathbb{B}_{ij}^{\tau T}P_1\end{bmatrix}$$

$$\pounds_{15}=[(I-\bar{\beta})\mathbb{B}_{ij}^{oeT}P_1\quad -\theta_2\mathbb{B}_{ij}^{oeT}P_1\quad 0\quad 0]$$

$$\pounds_{16}=\begin{bmatrix}\bar{\alpha}\bar{\beta}\mathbb{B}_{ij}^{eT}P_1 & \theta_2\bar{\alpha}\mathbb{B}_{ij}^{eT}P_1 & \theta_1\bar{\beta}\mathbb{B}_{ij}^{eT}P_1 & \theta_1\theta_2\mathbb{B}_{ij}^{eT}P_1\end{bmatrix}$$

$$\pounds_{17}=\begin{bmatrix}\mathbb{B}_{\omega i}^T & 0 & 0 & 0\end{bmatrix}$$

$$\pounds_{18}=\begin{bmatrix}(I-\bar{\alpha})\bar{\beta}\mathbb{B}_{ij}^{fT}P_1 & \theta_2(I-\bar{\alpha})\mathbb{B}_{ij}^{fT}P_1\\ -\theta_1\bar{\beta}\mathbb{B}_{ij}^{fT}P_1 & -\theta_1\theta_2\mathbb{B}_{ij}^{fT}P_1\end{bmatrix}$$

$$H_1=[I_{nx},0_{nx}],H_2=[0_{nx},I_{nx}]$$

$$\Theta_2=\begin{bmatrix}\Xi_{21} & \Xi_{22} & \Xi_{24}\\ * & \Xi_{23} & 0\\ * & * & \Xi_{26}\end{bmatrix}$$

$$\Xi_{21}=\Phi_2+\jmath_2\Pi_2^T+\jmath_2\Pi_2$$

$$\Xi_{22}=\begin{bmatrix}\mathbb{A}_{ij}^{2T}P_2 & 0_{14nx} & \mathbb{B}_{\omega i}^TP_2 & 0_{2nx}\end{bmatrix}^T$$

$$\Xi_{23}=-P_2R_2^{-1}P_2$$

$$\Xi_{26}=diag\left\{-\jmath_2R_{21},-\jmath_2R_{21},-\jmath_2R_{22},-\jmath_2R_{22}\right\}$$

[ht]

$$\Phi_2=\begin{bmatrix}\pounds_{19} & 0 & 0 & \pounds_{20}\\ * & \pounds_{21} & 0 & 0\\ * & * & 0 & 0\\ * & * & * & 0\end{bmatrix}$$

$$\pounds_{19}=-2\zeta_2P_2+sym\left\{P_2\mathbb{A}_{ij}^2\right\}+Q_{21}+Q_{22}$$

$$\pounds_{20}=P_2\mathbb{B}_{\omega i},\pounds_{21}=diag\left\{0,-\jmath_2Q_{22},0,\jmath_2Q_{21}\right\}$$

$$\jmath_1=e^{-\zeta_1h},\jmath_2=e^{\zeta_2h}$$

$$\Pi_\delta=[M_\delta+N_\delta\quad -N_\delta+K_\delta\quad -K_\delta$$

$$-M_\delta+J_\delta\quad -J_\delta\quad 0_{8nx}]$$

$$\Xi_{\delta4}=[M_\delta\quad J_\delta\quad N_\delta\quad K_\delta]$$

$$M_\delta=[M_{\delta1}^T\quad 0\quad 0\quad M_{\delta4}^T\quad 0\quad 0\quad 0\quad 0\quad 0]^T$$

$$J_\delta=[0\quad 0\quad 0\quad J_{\delta4}^T\quad J_{\delta5}^T\quad 0\quad 0\quad 0\quad 0]^T$$

$$N_\delta=[N_{\delta1}^T\quad N_{\delta2}^T\quad 0\quad 0\quad 0\quad 0\quad 0\quad 0\quad 0]^T$$

$$K_\delta=[0\quad K_{\delta2}^T\quad K_{\delta3}^T\quad 0\quad 0\quad 0\quad 0\quad 0\quad 0]^T$$

proof:According to the above requirements,choose the following Lyapunov-Krasovskii function as

$$\begin{aligned}V_\delta=&\eta^T(t)P_\delta\eta(t)+\int_{t-\tau_M}^t\eta^T(s)\vartheta_\delta(s)Q_{\delta1}\eta(s)ds\\&+\int_{t-o_M}^t\eta^T(s)\vartheta_\delta(s)Q_{\delta2}\eta(s)ds\\&+\int_{-\tau_M}^0\int_{t+\theta}^t\dot{\eta}^T(s)\vartheta_\delta(s)R_{\delta1}\dot{\eta}(s)dsd\theta\\&+\int_{-o_M}^0\int_{t+\theta}^t\dot{\eta}^T(s)\vartheta_\delta(s)R_{\delta2}\dot{\eta}(s)dsd\theta\end{aligned}\tag{35}$$

where $\vartheta=e^{2(-1)^\delta\zeta_\delta(t-s)},P_\delta>0,Q_{\delta1}>0,Q_{\delta2}>0,$ $P_{\delta1}>0,P_{\delta2}>0$,and δ is two time periods.When $\delta=$

1,DoS attack does not occur,the calculation of (32) can be obtained as follows

$$\begin{aligned}E\left\{\dot{V}_1(t)\right\} \leq & 2\zeta_1 V_1(t)+2\zeta_1\eta^T(t)P_1\eta(t)\\ &+2E\left\{\eta^T(t)P_1\eta(t)\right\}+\eta^T(t)(Q_{11}+Q_{12})\eta(t)\\ &-\eta^T(t-\tau_M)e^{-2\zeta_1 h}Q_{11}\eta(t-\tau_M)\\ &-\eta^T(t-o_M)e^{-2\zeta_1 h}Q_{12}\eta(t-o_M)\\ &+E\left\{\dot{\eta}^T(t)(R_{11}+R_{12})\dot{\eta}(t)\right\}\\ &-\int_{t-\tau(t)}^{t}\dot{\eta}^T(s)e^{-2\zeta_1 h}R_{11}\dot{\eta}(s)ds\\ &-\int_{t-\tau_M}^{t-\tau(t)}\dot{\eta}^T(s)e^{-2\zeta_1 h}R_{11}\dot{\eta}(s)ds\\ &-\int_{t-o(t)}^{t}\dot{\eta}^T(s)e^{-2\zeta_1 h}R_{12}\dot{\eta}(s)ds\\ &-\int_{t-o_M}^{t-o(t)}\dot{\eta}^T(s)e^{-2\zeta_1 h}R_{12}\dot{\eta}(s)ds\end{aligned} \tag{36}$$

Since the maximum delay of event-triggering and replay attacks does not exceed the sampling period h, there is $0 \leq \tau_M < h$ and $0 \leq o_M < h$.Then,according to [30], the free matrix is used to process (33).

$$\begin{aligned}&2\varsigma^T(t)M_1[\eta(t)-\eta(t-\tau(t))-\int_{t-\tau(t)}^{t}\dot{\eta}(s)ds]=0\\ &2\varsigma^T(t)J_1[\eta(t-\tau(t))-\eta(t-\tau_M)-\int_{t-\tau_M}^{t-\tau(t)}\dot{\eta}(s)ds]=0\\ &2\varsigma^T(t)N_1[\eta(t)-\eta(t-o(t))-\int_{t-o(t)}^{t}\dot{\eta}(s)ds]=0\\ &2\varsigma^T(t)K_1[\eta(t-o(t))-\eta(t-o_M)-\int_{t-o_M}^{t-o(t)}\dot{\eta}(s)ds]=0\end{aligned} \tag{37}$$

where M_1, J_1, N_1,and K_1 are the free weighting matrices,and $\varsigma(t)=\left[\eta^T(t)\quad \eta^T(t-o(t))\quad \eta^T(t-o_M)\right.$ $\left.\eta^T(t-\tau(t))\quad \eta^T(t-\tau_M)\quad e^T(t-o(t))\quad e^T(t)\quad \omega^T(t)\right.$ $\left.f^T(t)\right]^T$.Then,lemma 1 gives us the following

$$\begin{aligned}&-2\varsigma^T(t)M_1\int_{t-\tau(t)}^{t}\dot{\eta}(s)ds\\ &\leq -2e^{-2\zeta_1\tau_M}\varsigma^T M_1\int_{t-\tau(t)}^{t}\dot{\eta}(s)ds\\ &\leq e^{-2\zeta\tau_M}\varsigma^T(t)M_1R_{11}^{-1}M_1^T\varsigma(t)\\ &+e^{-2\zeta_1\tau_M}\int_{t-\tau(t)}^{t}\dot{\eta}^T(s)R_{11}\dot{\eta}(s)ds\end{aligned} \tag{38}$$

Combining (34) and (35),and other things as well,the single integral term in (33) can be obtained as

$$\begin{aligned}&-\int_{t-\tau(t)}^{t}\dot{\eta}^T(s)e^{-2\zeta_1\tau_M}R_{11}\dot{\eta}(s)ds\\ &\leq 2e^{-2\zeta_1\tau_M}\left[\eta(t)-\eta(t-\tau(t))\right]\\ &+e^{-2\zeta_1\tau_M}\varsigma^T(t)M_1R_{11}^{-1}M_1^T\varsigma(t)\end{aligned} \tag{39}$$

$$\begin{aligned}&-\int_{t-\tau_M}^{t-\tau(t)}\dot{\eta}^T(s)e^{-2\zeta_1\tau_M}R_{11}\dot{\eta}(s)ds\\ &\leq 2e^{-2\zeta_1\tau_M}\left[\eta(t-\tau(t))-\eta(t-\tau_M)\right]\\ &+e^{-2\zeta_1\tau_M}\varsigma^T(t)J_1R_{11}^{-1}J_1^T\varsigma(t)\end{aligned} \tag{40}$$

$$\begin{aligned}&-\int_{t-o(t)}^{t}\dot{\eta}^T(s)e^{-2\zeta_1 o_M}R_{12}\dot{\eta}(s)ds\\ &\leq 2e^{-2\zeta_1 o_M}\left[\eta(t)-\eta(t-o(t))\right]\\ &+e^{-2\zeta_1 o_M}\varsigma^T(t)N_1R_{12}^{-1}N_1^T\varsigma(t)\end{aligned} \tag{41}$$

$$\begin{aligned}&-\int_{t-o_M}^{t-o(t)}\dot{\eta}^T(s)e^{-2\zeta_1 o_M}R_{12}\dot{\eta}(s)ds\\ &\leq 2e^{-2\zeta_1 o_M}\left[\eta(t-o(t))-\eta(t-o_M)\right]\\ &+e^{-2\zeta_1 o_M}\varsigma^T(t)J_1R_{12}^{-1}J_1^T\varsigma(t)\end{aligned} \tag{42}$$

In order to distinguish, the original data is used instead of sampling time h.Then dealing with indeterminate data, we have the following

$$E\left\{\eta^T(t)P_1\eta^T\right\}=\eta^T(t)P_1\mathfrak{A} \tag{43}$$

$$\begin{aligned}E\left\{\dot{\eta}^T(t)R_1\dot{\eta}(t)\right\}=&\mathfrak{A}^TR_1\mathfrak{A}+\theta_2^2\mathfrak{B}^TR_1\mathfrak{B}\\ &+\theta_1^2\mathfrak{C}^TR_1\mathfrak{C}+\theta_1^2\theta_2^2\mathfrak{D}^TR_1\mathfrak{D}\end{aligned} \tag{44}$$

where

$$\begin{aligned}&R_1=R_{11}+R_{12}\\ &\mathfrak{A}=\mathbb{A}_{ij}^1\eta(t)+\mathbb{B}_{\omega i}\omega(t)+(I-\bar{\alpha})\bar{\beta}\mathbb{B}_{ij}^f f(t)\\ &+(I-\bar{\beta})\mathbb{B}_{ij}^o\eta(t-o(t))+(I-\bar{\beta})\mathbb{B}_{ij}^{oe}e(t-o(t))\\ &+\bar{\alpha}\bar{\beta}\mathbb{B}_{ij}^{\tau}\eta(t-\tau(t))+\bar{\alpha}\bar{\beta}\mathbb{B}_{ij}^{e}e(t)\\ &\mathfrak{B}=\mathbb{B}_{ij}^o\eta(t-o(t))+(I-\bar{\alpha})\mathbb{B}_{ij}^f f(t)\end{aligned}$$

$$+\bar{\alpha}\mathbb{B}_{ij}^{\tau}\eta(t-\tau(t))+\bar{\alpha}\mathbb{B}_{ij}^{e}e(t)-\mathbb{B}_{ij}^{oe}e(t-o(t))$$
$$\mathfrak{C}=-\bar{\beta}\mathbb{B}_{ij}^{f}f(t)+\bar{\beta}\mathbb{B}_{ij}^{\tau}\eta(t-\tau(t))+\bar{\beta}\mathbb{B}_{ij}^{e}e(t)$$
$$\mathfrak{D}=-\mathbb{B}_{ij}^{f}f(t)+\mathbb{B}_{ij}^{e}e(t)+\mathbb{B}_{ij}^{\tau}\eta(t-\tau(t))$$

According to the event-triggered (13), we can obtain

$$\begin{aligned}&(\sigma_s-1)e^T(t)H_1^TC^T\Omega_sCH_1e(t)\\&+\sigma_s\eta^T(t-\tau(t))H_1^TC^T\Omega_sCH_1\eta(t-\tau(t))>0\end{aligned}\tag{45}$$

$$\begin{aligned}&(\sigma_c-1)e^T(t)H_2^T\Omega_cH_2e(t)\\&+\sigma_c\eta^T(t-\tau(t))H_2^T\Omega_cH_2\eta(t-\tau(t))>0\end{aligned}\tag{46}$$

Based on Assumption 4 of deception attacks, we have the following equation

$$\begin{aligned}(CH_1(\eta(t-\tau(t))+e(t)))^TF_s^TF_s(CH_1(\eta(t-\tau(t))+e(t)))\\-f^T(t)H_1^TH_1f(t)\geq0\end{aligned}\tag{47}$$

$$\begin{aligned}(H_2(\eta(t-\tau(t))+e(t)))^TF_c^TF_c(H_2(\eta(t-\tau(t))+e(t)))\\-f^T(t)H_2^TH_2f(t)\geq0\end{aligned}\tag{48}$$

By combining (33)-(45) and Schur complement lemma,it yields

$$E\left\{\dot{V}_1(t)\right\}\leq-2\zeta_1V_1(t)+\varsigma^T(t)\Theta_1\varsigma(t)$$

Meanwhile, as a result of (27), the following inequality can be finally obtained

$$E\left\{\dot{V}_1(t)\right\}\leq-2\zeta_1V_1(t)\tag{49}$$

Similarly, for $\delta=2$, (32) becomes

$$\begin{aligned}E\left\{\dot{V}_2(t)\right\}\leq&2\zeta_1V_2(t)+2\zeta_1\eta^T(t)P_2\eta(t)\\&+2E\left\{\eta^T(t)P_2\eta(t)\right\}+\eta^T(t)(Q_{21}+Q_{22})\eta(t)\\&-\eta^T(t-\tau_M)e^{-2\zeta_1h}Q_{21}\eta(t-\tau_M)\\&-\eta^T(t-o_M)e^{-2\zeta_1h}Q_{21}\eta(t-o_M)\\&+2e^{2\zeta_2\tau_M}\varsigma^T(t)M_2(\eta(t)-\eta(t-\tau(t)))\\&+2e^{2\zeta_2\tau_M}\varsigma^T(t)J_2(\eta(t-\tau(t))-\eta(t-\tau_M))\\&+2e^{2\zeta_2o_M}\varsigma^T(t)N_2(\eta(t)-\eta(t-o(t)))\\&+2e^{2\zeta_2o_M}\varsigma^T(t)K_2(\eta(t-o(t))-\eta(t-o_M))\\&+2e^{2\zeta_2\tau_M}\varsigma^T(t)M_2R_{21}^{-1}M_2^T\varsigma(t)\\&+2e^{2\zeta_2\tau_M}\varsigma^T(t)J_2R_{21}^{-1}J_2^T\varsigma(t)\\&+2e^{2\zeta_2o_M}\varsigma^T(t)N_2R_{22}^{-1}N_2^T\varsigma(t)\\&+2e^{2\zeta_2o_M}\varsigma^T(t)K_2R_{22}^{-1}K_2^T\varsigma(t)\\&+\eta^T(t)\mathbb{A}_{ij}^{2T}R_2\mathbb{A}_{ij}^{2}\eta(t)+\eta^T(t)\mathbb{A}_{ij}^{2T}R_2\mathbb{B}_{\omega i}\omega(t)\\&+\omega^T(t)\mathbb{B}_{\omega i}^{T}R_2\mathbb{A}_{ij}^{2}\eta(t)+\omega^T(t)\mathbb{B}_{\omega i}^{T}R_2\mathbb{B}_{\omega i}\omega(t)\end{aligned}$$

Again using the Schuer complement, (47) is converted to

$$E\left\{\dot{V}_2(t)\right\}\leq2\zeta_2V_2(t)+\varsigma^T(t)\Theta_2\varsigma(t)$$

Similarly, by using (27), we can get the final $V_2(t)$ is

$$E\left\{\dot{V}_2(t)\right\}\leq2\zeta_2V_2(t)\tag{51}$$

Then,it can be obtained

$$\begin{cases}E\left\{V_1(t)\right\}\leq e^{-2\zeta_1(t-\mathfrak{l}^n)}E\left\{V_1(\mathfrak{l}^n)\right\}, & t\in\mathcal{L}_1^n\\E\left\{V_2(t)\right\}\leq e^{2\zeta_2(t-\mathfrak{l}^n-\mathfrak{s}^n)}E\left\{V_2(\mathfrak{l}^n+\mathfrak{s}^n)\right\}, & t\in\mathcal{L}_2^n\end{cases}\tag{52}$$

Combine (28)-(32) to obtain

$$\begin{cases}E\left\{V_1(\mathfrak{l}^n)\right\}\leq\partial_2E\left\{V_2((\mathfrak{l}^n)^-)\right\}\\E\left\{V_2(\mathfrak{l}^n+\mathfrak{s}^n)\right\}\leq\partial_1e^{2(\zeta_1+\zeta_2)h}E\left\{V_1((\mathfrak{l}^n+\mathfrak{s}^n)^-)\right\}\end{cases}\tag{53}$$

Then,for $t=[\mathfrak{l}^n,\mathfrak{l}^n+\mathfrak{s}^n)$,combining (49) ,(50),and Assumption 2 can be obtained

$$\begin{aligned}&E\left\{V_1(t)\right\}\\&\leq\partial_2e^{-2\zeta_1(t-\mathfrak{l}^n)}E\left\{V_2((\mathfrak{l}^n)^-)\right\}\\&\leq\partial_2e^{-2\zeta_1(t-\mathfrak{l}^n)}e^{2\zeta_2(t-\mathfrak{l}^{n-1}-\mathfrak{s}^{n-1})}E\left\{V_2(\mathfrak{l}^{n-1}-\mathfrak{s}^{n-1})\right\}\\&\leq\partial_1\partial_2e^{2(\zeta_1+\zeta_2)h}e^{-2\zeta_1s_{min}}e^{2\zeta_2d_{max}}E\left\{V_1((\mathfrak{l}^{n-1}-\mathfrak{s}^{n-1})^-)\right\}\end{aligned}\tag{54}$$

$$\vdots$$

$$\leq (\partial_1\partial_2)^n e^{2n(\zeta_1+\zeta_2)h} e^{-2n\zeta_1 s_{min}} e^{2n\zeta_2 d_{max}} E\left\{V_1(0)\right\}$$

For $t = [\mathfrak{l}^n, \mathfrak{l}^n + \mathfrak{s}^n)$,according to Assumption 3,$n \leq \hbar_1 + (t/\hbar_2)$ The limitations of DoS attacks can be obtained as follows

$$E\left\{V_1(t)\right\} \leq e^{\nu_1} e^{-\check{\nu}t} E\left\{V_1(0)\right\} \tag{55}$$

where

$$\nu_1 = \hbar_1 \left(2(\zeta_1+\zeta_2)h - 2\zeta_1 s_{min} + 2\zeta_2 d_{max} + ln(\partial_1\partial_2)\right)$$

$$\nu = \frac{1}{\hbar_2}\left(-2(\zeta_1+\zeta_2)h + 2\zeta_1 s_{min} - 2\zeta_2 d_{max} - \frac{1}{2} ln(\partial_1\partial_2)\right)$$

Then we do the same iteration for $V_2(t)$,here $\leq \hbar_1 + (t/\hbar_2) < n+1$

$$E\left\{V_2(t)\right\} \leq \frac{1}{\partial_2} e^{\nu_2} e^{-\check{\nu}t} E\left\{V_1(0)\right\} \tag{56}$$

where

$$\nu_2 = (\hbar_2 + 1)\left(2(\zeta_1+\zeta_2)h - 2\zeta_1 s_{min} + 2\zeta_2 d_{max} + ln(\partial_1\partial_2)\right)$$

Defining $\mathfrak{M} = max\left\{e^{\nu_1}, \frac{1}{\partial_2} e^{\nu_2}\right\}$

$$E\left\{V(t)\right\} \leq \mathfrak{M} e^{-\check{\nu}t} E\left\{V_1(0)\right\} \tag{57}$$

Based on the above analysis, we get the following formula:

$$E\left\{V(t)\right\} \geq \mathfrak{f}_1 \left\|\eta(t)\right\|^2, E\left\{V_1(0)\right\} \leq \mathfrak{f}_2 \left\|\eta_0\right\|_h^2 \tag{58}$$

where $\mathfrak{f}_1 = min\left\{\lambda_{min}(P_\delta)\right\}, \mathfrak{f}_2 = max\left\{\lambda_{max}(P_\delta) + h\lambda_{max}(Q_{\delta 1} + Q_{\delta 2}) + (h^2/2)\lambda_{max}(R_{\delta 1} + R_{\delta 2})\right\}$

Then,combining (54) with (55),we can get

$$\left\|\eta(t)\right\| \leq \sqrt{\frac{\mathfrak{M}\mathfrak{f}_2}{\mathfrak{f}_1}} e^{-\frac{\nu}{2}t} \left\|\eta_0\right\|_h \tag{59}$$

Then the stability of system (25) is based on conditions (27)-(31).

We define $\Psi_\delta(t) = E\left\{\dot{V}_\delta(t)\right\} + z^T(t)z(t) - \check{\gamma}^2\omega^T(t)\omega(t)$. According to [25],we can set $\Psi_\delta(t) < 2(-1)^\delta \zeta_\delta V_\delta(t)$ is true,then we can get the following formula:

$$\sum_{i=1}^{2}\sum_{j=1}^{2} \chi_i\chi_j \varsigma^T(t)\Theta_{ij}^\delta \varsigma(t) < 0 \tag{60}$$

A relaxation matrix $\mathfrak{S}_i^\delta$,where $\sum_{i=1}^{2}\sum_{j=1}^{2} \chi_i(\beth_j - \chi_j)\mathfrak{S}_i^\delta$ is introduced here to achieve the aim of relaxing the conditions.

$$\begin{aligned}\sum_{i=1}^{2}\sum_{j=1}^{2}\chi_i\chi_j\varsigma^T(t)\Theta_{ij}^\delta\varsigma(t) = \frac{1}{2}\sum_{i=1}^{2}\sum_{j=1}^{2}\chi_i\varsigma^T(t)\left[(\chi_j - \kappa_j\beth_j)\right.\\ (\Theta_{ij}^\delta + \Theta_{ji}^\delta - \mathfrak{S}_i^\delta - \mathfrak{S}_j^\delta) + \beth_j(\kappa_j\Theta_{ij}^\delta + \kappa_i\Theta_{ji}^\delta - \kappa_j\mathfrak{S}_i^\delta\\ \left.-\kappa_i\mathfrak{S}_j^\delta + \mathfrak{S}_i^\delta + \mathfrak{S}_j^\delta)\right]\varsigma(t)\end{aligned} \tag{61}$$

Combining with (28) and (29),then we can obtain

$$E\left\{\dot{V}_\delta(t)\right\} - 2(-1)^\delta\zeta_\delta V_\delta(t) + z^T(t)z(t) - \gamma^2\omega^T(t)\omega(t) \leq 0 \tag{62}$$

So for all of the $t \in \left[0, \mathfrak{l}^{n+1}\right)$, by (51) and (52),we get

$$\begin{aligned}&\sum_{m=0}^{n}\int_{\mathfrak{l}^n}^{\mathfrak{l}^n+\mathfrak{s}^n} e^{-2\zeta_1(\mathfrak{l}^m - t)}(E\left\{\dot{V}_1(t)\right\} + 2\zeta_1 V_1(t))dt\\ &+\sum_{m=0}^{n}\int_{\mathfrak{l}^n+\mathfrak{s}^n}^{\mathfrak{l}^{n+1}} \partial_2 e^{2\zeta_2(\mathfrak{l}^{m+1}-t)}(E\left\{\dot{V}_2(t)\right\} + 2\zeta_2 V_2(t))dt\\ &=\sum_{m=0}^{n}[e^{2\zeta_1\mathfrak{s}^m}E\left\{V_1(\mathfrak{l}^m+\mathfrak{s}^m)^-\right\} - E\left\{V_1(t)\right\}\\ &-\partial_2 e^{2\zeta_2(\mathfrak{l}^{m+1}-\mathfrak{l}^m-\mathfrak{s}^m)}E\left\{V_2(\mathfrak{l}^m+\mathfrak{s}^m)^-\right\} + \partial_2 E\left\{V_2(\mathfrak{l}^{m+1})\right\}]\\ &\geq\sum_{m=0}^{n}[(\frac{1}{\partial_1}e^{-2(\zeta_1+\zeta_2)h+2\zeta_1\mathfrak{s}^m} - \partial_2 e^{2\zeta_2(\mathfrak{l}^{m+1}-\mathfrak{l}^m-\mathfrak{s}^m)})\\ &V_2(\mathfrak{l}^m+\mathfrak{s}^m)] + (V_1(\mathfrak{l}^{n+1}) - V_1(0))\end{aligned} \tag{63}$$

Combine (61) with (62) and because of $-\partial_2 e^{2\zeta_2 d_{max}} + (1/\partial_1)e^{-2(\zeta_1+\zeta_2)h+2\zeta_1 s_{min}} > 0$, then when $V_1(0) = 0$, we get the following

$$\sum_{m=0}^{n}\int_{\mathfrak{l}^n}^{\mathfrak{l}^n+\mathfrak{s}^n} min\left\{1,\partial_2\right\} z^T(t)z(t)dt$$
$$< \sum_{m=0}^{n}\int_{\mathfrak{l}^n}^{\mathfrak{l}^n+\mathfrak{s}^n} max\left\{e^{2\zeta_1 s_{max}}, e^{2\zeta_2 d_{max}}\right\}\gamma^2\omega^T(t)\omega(t)dt \tag{64}$$

Furtheremore,by (63) and the definition, we hava

$$\int_0^\infty z^T(t)z(t) < \int_0^\infty \breve{\gamma}^2\omega^T(t)\omega(t) \tag{65}$$

where $\breve{\gamma} = \gamma\sqrt{\breve{\gamma}_1/\breve{\gamma}_2}, \breve{\gamma}_1 = max\left\{e^{2\zeta_1 s_{max}}, e^{2\zeta_2 d_{max}}\right\}$,and $\breve{\gamma}_2 = min\left\{1,\partial_2\right\}$,for system (25), H^∞ performance is stable,this completes the proof.

Remark 5:Since the dynamic system of the vhicle is strictly followed in this paper, the range of parameters that can be modified in the system is small. Relaxation matrix is introduced here to make the system more stable. Also for γ performance parameters more detailed.

Theorem 2:System (25) has been proved stable in theorem 1, then for given scalars $\tau_M, o_M, \bar{\alpha}_s, \bar{\alpha}_c, \bar{\beta}_s, \bar{\beta}_c, \theta_{s1}, \theta_{c1}, \theta_{s2}, \theta_{c2}, \iota, \Bbbk, s_{min}, d_{max}$.If there is a positive definite matrix $,\hat{\Omega}_s, \hat{\Omega}_c, X_1, X_2, \hat{Q}_{11}, \hat{Q}_{12}, \hat{Q}_{21}, \hat{Q}_{22}, \hat{R}_{11}, \hat{R}_{12}, \hat{R}_{21},$ and$\hat{R}_{22}$, $\hat{A}_j^{c\delta}, \hat{C}_j^c, \hat{L}_j^c$ to satisfy the controller and free matrices $\hat{M}_\delta, \hat{J}_\delta, \hat{N}_\delta, \hat{K}_\delta$, then it satisfies

$$\hat{\Theta}_{ij}^\delta + \hat{\Theta}_{ji}^\delta - \hat{\mathfrak{S}}_i^\delta - \hat{\mathfrak{S}}_j^\delta < 0 \tag{66}$$

$$\kappa_j\hat{\Theta}_{ij}^\delta + \kappa_i\hat{\Theta}_{ji}^\delta - \kappa_j\hat{\mathfrak{S}}_i^\delta - \kappa_i\hat{\mathfrak{S}}_j^\delta + \hat{\mathfrak{S}}_i^\delta + \hat{\mathfrak{S}}_j^\delta < 0 \tag{67}$$

where

$$\hat{\Theta}_{ij}^1 = \begin{bmatrix} \hat{\Theta}_1 & \Re_{ij} & H_3 \\ * & -\Bbbk^{-1}\iota^{-2}I & 0 \\ * & * & -\Bbbk I \end{bmatrix}$$

$$\hat{\Theta}_1 = \begin{bmatrix} \hat{\Xi}_{11} & \Xi_{12} & \hat{\Xi}_{13} & \hat{\Xi}_{14} & \Xi_{15} \\ * & \Xi_{16} & 0 & 0 & 0 \\ * & * & \hat{\Xi}_{17} & 0 & 0 \\ * & * & * & \hat{\Xi}_{18} & 0 \\ * & * & * & * & -I \end{bmatrix}$$

$$\hat{\Xi}_{11} = \hat{\Phi}_1 + \jmath_1\hat{\Pi}_1^T + \jmath_1\hat{\Pi}_1, \Xi_{16} = diag\left\{I, I\right\}$$
$$\Xi_{12} = \begin{bmatrix} 0 & 0 & 0 & \pounds_{10}^T & 0 & 0 & \pounds_{11}^T & 0 & 0 \end{bmatrix}^T$$
$$\hat{\Xi}_{13} = \begin{bmatrix} \hat{\pounds}_{12}^T & \hat{\pounds}_{13}^T & 0 & \hat{\pounds}_{14}^T & 0 & \hat{\pounds}_{15}^T \\ & & & \hat{\pounds}_{16}^T & \hat{\pounds}_{17}^T & \hat{\pounds}_{18}^T \end{bmatrix}^T$$
$$\Xi_{15} = [X_1 D_i H_1 \quad 0 \quad 0 \quad 0 \quad 0 \quad 0 \quad 0 \quad 0 \quad 0]^T$$
$$\hat{\Xi}_{17} = diag\left\{-2\mathfrak{e}_1 X_1 + \mathfrak{e}_1^2\hat{R}_1, -2\mathfrak{e}_1 X_1 + \mathfrak{e}_1^2\hat{R}_1 \right.$$
$$\left. -2\mathfrak{e}_1 X_1 + \mathfrak{e}_1^2\hat{R}_1, -2\mathfrak{e}_1 X_1 + \mathfrak{e}_1^2\hat{R}_1\right\}$$
$$\hat{\Xi}_{18} = diag\left\{-\jmath_1\hat{R}_{11}, -\jmath_1\hat{R}_{11}, -\jmath_1\hat{R}_{12}, -\jmath_1\hat{R}_{12}\right\}$$
$$\hat{\Phi}_1 = \begin{bmatrix} \hat{\pounds}_1 & \hat{\pounds}_2 & \hat{\pounds}_3 & \hat{\pounds}_4 & \hat{\pounds}_5 \\ * & \hat{\pounds}_6 & 0 & 0 & 0 \\ * & * & \hat{\pounds}_7 & 0 & 0 \\ * & * & * & \pounds_8 & 0 \\ * & * & * & * & \pounds_9 \end{bmatrix}$$
$$\hat{\pounds}_1 = 2\zeta_1 X_1 + sym\left\{\hat{\mathbb{A}}_{ij}^1\right\} + \hat{Q}_{11} + \hat{Q}_{12}$$
$$\pounds_2 = \begin{bmatrix} (I-\bar{\beta})\hat{\mathbb{B}}_{ij}^o & 0 & \bar{\alpha}\bar{\beta}\hat{\mathbb{B}}_{ij}^\tau & 0 \end{bmatrix}$$
$$\pounds_3 = \begin{bmatrix} (I-\bar{\beta})\hat{\mathbb{B}}_{ij}^{oe} & \bar{\alpha}\bar{\beta}\hat{\mathbb{B}}_{ij}^e \end{bmatrix}$$
$$\pounds_4 = \hat{\mathbb{B}}_{\omega i}, \pounds_5 = (I-\bar{\alpha})\bar{\beta}\hat{\mathbb{B}}_{ij}^f$$
$$\pounds_6 = diag\left\{\sigma_s H_1^T C^T\hat{\Omega}_s C H_1 + \sigma_c H_2^T\hat{\Omega}_c H_2, -\jmath_1\hat{Q}_{12}, \right.$$
$$\left.\sigma_s H_1^T C^T\hat{\Omega}_s C H_1 + \sigma_c H_2^T\hat{\Omega}_c H_2, -\jmath_1\hat{Q}_{11}\right\}$$
$$\pounds_7 = diag\left\{(\sigma_s-1)H_1^T C^T\hat{\Omega}_s C H_1 + (\sigma_c-1)H_2^T\hat{\Omega}_c H_2, \right.$$
$$\left.(\sigma_s-1)H_1^T C^T\hat{\Omega}_s C H_1 + (\sigma_c-1)H_2^T\hat{\Omega}_c H_2\right\}$$
$$\pounds_8 = -\gamma^2 I, \pounds_9 = diag\left\{-H_1^T H_1 - H_2^T H_2\right\}$$
$$\pounds_{11} = [F_s^T C^T H_1^T \quad F_c^T H_2^T], \pounds_{11} = \pounds_{10}$$
$$\pounds_{12} = [\hat{\mathbb{A}}_{ij}^{1T} \quad 0 \quad 0 \quad 0]$$
$$\pounds_{13} = [(I-\bar{\beta})\hat{\mathbb{B}}_{ij}^{oT} \quad -\theta_2\hat{\mathbb{B}}_{ij}^{oT}]$$
$$\pounds_{14} = \begin{bmatrix} \bar{\alpha}\bar{\beta}\hat{\mathbb{B}}_{ij}^{\tau T} & \theta_2\bar{\alpha}\hat{\mathbb{B}}_{ij}^{\tau T} & \theta_1\bar{\beta}\hat{\mathbb{B}}_{ij}^{\tau T} & \theta_1\theta_2\hat{\mathbb{B}}_{ij}^{\tau T} \end{bmatrix}$$
$$\pounds_{15} = [(I-\bar{\beta})\hat{\mathbb{B}}_{ij}^{oeT} \quad -\theta_2\hat{\mathbb{B}}_{ij}^{oeT} \quad 0 \quad 0]$$
$$\pounds_{16} = \begin{bmatrix} \bar{\alpha}\bar{\beta}\hat{\mathbb{B}}_{ij}^{eT} & \theta_2\bar{\alpha}\hat{\mathbb{B}}_{ij}^{eT} & \theta_1\bar{\beta}\hat{\mathbb{B}}_{ij}^{eT} & \theta_1\theta_2\hat{\mathbb{B}}_{ij}^{eT} \end{bmatrix}$$
$$\pounds_{17} = \begin{bmatrix} \hat{\mathbb{B}}_{\omega i}^T & 0 & 0 & 0 \end{bmatrix}$$

$$\pounds_{18} = \Big[(I-\bar{\alpha})\bar{\beta}\hat{\mathbb{B}}_{ij}^{fT} \quad \theta_2(I-\bar{\alpha})\hat{\mathbb{B}}_{ij}^{fT} \quad -\theta_1\bar{\beta}\hat{\mathbb{B}}_{ij}^{fT} \quad -\theta_1\theta_2\hat{\mathbb{B}}_{ij}^{fT}\Big]$$

$$H_1 = [I_{nx}, 0_{nx}], H_2 = [0_{nx}, I_{nx}]$$

$$H_3 = [0 \quad 0 \quad 0 \quad I \quad 0 \quad 0 \quad I \quad 0_{26nx}]$$

$$\Re = [\bar{\alpha}\bar{\beta}\hat{\mathbb{B}}_{ij}^{\Delta T} \quad 0_{20nx} \quad \bar{\alpha}\bar{\beta}\hat{\mathbb{B}}_{ij}^{\Delta T} \quad \theta_2\bar{\alpha}\hat{\mathbb{B}}_{ij}^{\Delta T} \quad \theta_1\bar{\beta}\hat{\mathbb{B}}_{ij}^{\Delta T} \quad \theta_1\theta_2\hat{\mathbb{B}}_{ij}^{\Delta T} \quad 0_{10nx}]$$

$$\hat{\Theta}_{ij}^2 = \hat{\Theta}_2$$

$$\hat{\Theta}_2 = \begin{bmatrix} \hat{\Xi}_{21} & \hat{\Xi}_{22} & \hat{\Xi}_{24} & \Xi_{25} \\ * & \hat{\Xi}_{23} & 0 & 0 \\ * & * & \hat{\Xi}_{26} & 0 \\ * & * & * & -I \end{bmatrix}$$

$$\hat{\Xi}_{21} = \hat{\Phi}_2 + \jmath_2\hat{\Pi}_2^T + \jmath_2\hat{\Pi}_2$$

$$\hat{\Xi}_{22} = \Big[\hat{\mathbb{A}}_{ij}^2 \quad 0_{14nx} \quad \hat{\bar{\mathbb{B}}}_{\omega i} \quad 0_{2nx}\Big]^T$$

$$\hat{\Xi}_{23} = -2\mathfrak{e}_2X_2 + \mathfrak{e}_2^2\hat{R}_2, \Xi_{25} = \Xi_{15}$$

$$\hat{\Xi}_{26} = diag\Big\{-\jmath_2\hat{R}_{21}, -\jmath_2\hat{R}_{21}, -\jmath_2\hat{R}_{22}, -\jmath_2\hat{R}_{22}\Big\}$$

$$\Phi_2 = \begin{bmatrix} \hat{\pounds}_{19} & 0 & 0 & \hat{\pounds}_{20} \\ * & \hat{\pounds}_{21} & 0 & 0 \\ * & * & 0 & 0 \\ * & * & * & 0 \end{bmatrix}$$

$$\pounds_{19} = -2\zeta_2X_2 + sym\Big\{\hat{\mathbb{A}}_{ij}^2\Big\} + \hat{Q}_{21} + \hat{Q}_{22}$$

$$\pounds_{20} = \hat{\bar{\mathbb{B}}}_{\omega i}, \pounds_{21} = diag\Big\{0, -\jmath_2\hat{Q}_{22}, 0, \jmath_2\hat{Q}_{21}\Big\}$$

$$\jmath_1 = e^{-\zeta_1 h}, \jmath_2 = e^{\zeta_2 h}$$

$$\hat{\Pi}_\delta = \Big[\hat{M}_\delta + \hat{N}_\delta \quad -\hat{N}_\delta + \hat{K}_\delta \quad -\hat{K}_\delta \quad -\hat{M}_\delta + \hat{J}_\delta \quad -\hat{J}_\delta \quad 0_{8nx}\Big]$$

$$\hat{\Xi}_{\delta 4} = \Big[\hat{M}_\delta \quad \hat{J}_\delta \quad \hat{N}_\delta \quad \hat{K}_\delta\Big]$$

$$\hat{M}_\delta = [\hat{M}_{\delta 1}^T \quad 0 \quad 0 \quad \hat{M}_{\delta 4}^T \quad 0 \quad 0 \quad 0 \quad 0 \quad 0]^T$$

$$\hat{J}_\delta = [0 \quad 0 \quad 0 \quad \hat{J}_{\delta 4}^T \quad \hat{J}_{\delta 5}^T \quad 0 \quad 0 \quad 0 \quad 0]^T$$

$$\hat{N}_\delta = [\hat{N}_{\delta 1}^T \quad \hat{N}_{\delta 2}^T \quad 0 \quad 0 \quad 0 \quad 0 \quad 0 \quad 0 \quad 0]^T$$

$$\hat{K}_\delta = [0 \quad \hat{K}_{\delta 2}^T \quad \hat{K}_{\delta 3}^T \quad 0 \quad 0 \quad 0 \quad 0 \quad 0 \quad 0]^T$$

$$\hat{\mathbb{A}}_i j^1 = \begin{bmatrix} A_i\check{X}_1 & 0 \\ 0 & \hat{A}_j^{c1} \end{bmatrix}, \hat{\mathbb{A}}_i j^2 = \begin{bmatrix} A_i\check{X}_2 & 0 \\ 0 & \hat{A}_j^{c2} \end{bmatrix},$$

$$\hat{\mathbb{B}}_{ij}^o = \begin{bmatrix} 0 & B_{1i}\hat{C}_j^c \\ \hat{L}_j^cC & 0 \end{bmatrix},$$

$$\Delta = \begin{bmatrix} 0 & \Delta_g \\ \Delta_f & 0 \end{bmatrix}, \hat{\mathbb{B}}_{ij}^\Delta = \hat{\mathbb{B}}_{ij}^o = \hat{\mathbb{B}}_{ij}^{oe} = \hat{\mathbb{B}}_{ij}^f = \hat{\mathbb{B}}_{ij}^\tau = \hat{\mathbb{B}}_{ij}^e,$$

$$\hat{\mathbb{B}}_{\omega i} = \begin{bmatrix} B_{2i}\check{X}_1 \\ 0 \end{bmatrix}, \hat{\bar{\mathbb{B}}}_{\omega i} = \begin{bmatrix} B_{2i}\check{X}_2 \\ 0 \end{bmatrix}$$

Then the controller is obtained as

$$\hat{A}_j^{c1} = A_j^{c1}\check{X}_1, \hat{A}_j^{c2} = A_j^{c2}\check{X}_2, \hat{C}_j^c = C_j^c\check{X}_1$$
$$\hat{L}_j^c = L_j^c\check{X}_1, \hat{\Omega}_s = \check{X}_1^T\Omega_s\check{X}_1, \hat{\Omega}_c = \check{X}_1^T\Omega_c\check{X}_1$$

proof:By defining $X_\delta = P_\delta^{-1}$,and since the system coefficient needs to be subdivided, then $X_\delta = \begin{bmatrix} \check{X}_\delta & 0 \\ 0 & \check{X}_\delta \end{bmatrix}$,pre- and post-multiplying both side (30) and (31) by $\mathfrak{T} = diag\{X_1, X_1, X_1, X_1, X_1, X_1, X_1, I, X_1, I, I, X_1, X_1, X_1, X_1, I, I, I, I, I\}$.Then there is $\hat{A}_j^{c1} = A_j^{c1}\check{X}_1, \hat{A}_j^{c2} = A_j^{c2}\check{X}_2, \hat{C}_j^c = C_j^c\check{X}_1, \hat{L}_j^c = L_j^c\check{X}_1, \hat{\Omega}_s = \check{X}_1^T\Omega_s\check{X}_1, \hat{\Omega}_c = \check{X}_1^T\Omega_c\check{X}_1$,For Q_δ,and R_δ, after performing the contract transformation, define $\hat{Q}_{11} = X_1^TQ_{11}X_1, \hat{Q}_{12} = X_1^TQ_{12}X_1, \hat{Q}_{21} = X_2^TQ_{21}X_2$, $\hat{Q}_{22} = X_2^TQ_{22}X_2, \hat{R}_{11} = X_1^TR_{11}X_1, \hat{R}_{12} = X_1^TR_{12}X_1, \hat{R}_{21} = X_1^TR_{21}X_1, \hat{R}_{22} = X_1^TR_{22}X_1$.

Due to quantification exists in the absence of DoS attack time, we get the following inequation with lemma 2

$$\mathfrak{T}\Theta_{ij}^1\mathfrak{T} = \hat{\Theta}_1 + sym\{\Re^T\Delta H_3\} < 0 \tag{68}$$

where

$$H_3 = [0 \quad 0 \quad 0 \quad I \quad 0 \quad 0 \quad I \quad 0_{26nx}]$$
$$\Re = [\bar{\alpha}\bar{\beta}\hat{\mathbb{B}}_{ij}^{\Delta T} \quad 0_{20nx} \quad \bar{\alpha}\bar{\beta}\hat{\mathbb{B}}_{ij}^{\Delta T} \quad \theta_2\bar{\alpha}\hat{\mathbb{B}}_{ij}^{\Delta T} \quad \theta_1\bar{\beta}\hat{\mathbb{B}}_{ij}^{\Delta T} \quad \theta_1\theta_2\hat{\mathbb{B}}_{ij}^{\Delta T} \quad 0_{10nx}]$$

Then according to [26], and because of $\delta \in [-\iota, \iota]$, there exists a constant $\Bbbk > 0$, so that there is the following

$$sym\{\Re^T\Delta H_3\} \leq \Bbbk\iota^2\Re^T\Re + \Bbbk^{-1}H_3^TH_3 \tag{69}$$

And then using Schur complement, then (68) can be rewritten as

$$\begin{bmatrix} \hat{\Theta}_1 & \Re_{ij} & H_3 \\ * & -\mathbb{k}^{-1}\iota^{-2}I & 0 \\ * & * & -\mathbb{k}I \end{bmatrix} \tag{70}$$

Remark 6:Because of the property of quantization, it has an upper bound and a lower bound, which is used to adjust the accuracy of data transmission. So when you solve it, you can transform the variable to a fixed value by scaling it up.(68) refers to the amplification method in [26].

4. Simulations

This paper is based on the dynamics of vehicle, given the system, then the simulation is based on the vehicel given in the previous matlab simulation experiment, in order to illustrate the effectiveness of the designed output-feedback controller.

In the actual process, the general physical parameters of the vehicle is $m = 1500\mathsf{kg}, l_f = 1.156\mathsf{m}, l_r = 1.569\mathsf{m}$, the turning stiffness of the car can be positive or negative, here set as a positive constant $C_{\alpha f} = 87000\mathsf{N/rad}, C_{\alpha r} = 45000\mathsf{N/rad}$, the vehicle yaw inertia distance $I_z = 4500\mathsf{kg}\cdot\mathsf{m}^2$, under normal circumstances, the vehicle yaw speed is not big, so you can set $l_p = 0.4v_x, v_{x\ min} = 5\mathsf{m/s}, v_{x\ max} = 16\mathsf{m/s}$.

For general parameters, the parameters in the text are defined so that $\bar{\alpha}_s = 0.2, \bar{\alpha}_c = 0.2, \bar{\beta}_s = 0.3, \bar{\beta}_c = 0.3$, then $\theta_{s1} = \theta_{c1} = 0.16, \theta_{s2} = \theta_{c2} = 0.21$. Set event triggering parameters $h = 0.05, \sigma_s = 0.5, \sigma_c = 0.05$, and then we have $\zeta_1 = 0.3, \zeta_2 = 0.4, \partial_1 = 1.23, \partial_2 = 1.06, s_{max} = 40h, s_{min} = 21h, d_{max} = 5h, \iota = 0.784, \mathbb{k} = 15, \gamma = 1$,and finally, the coefficients of the relaxation matrix $\kappa_1 = 0.7, \kappa_2 = 0.9$ to ensure $\chi_j - \kappa_j \beth_j > 0$,then set the matrix of deception attacks upper limit $\mathcal{F}_s = diag\{3,2,1\}, \mathcal{F}_s = diag\{1,1,2,1\}$.So in order to solve theorem 2, the event trigger and controller gain are calculated as follows

$$\Omega_s = \begin{bmatrix} -26.7412 & 7.2710 & 4.0160 \\ -1.7271 & -6.1256 & -1.2894 \\ -5.8668 & 1.3119 & -26.5708 \end{bmatrix}$$

$$\Omega_s = \begin{bmatrix} 7.9234 & 1.5554 & -5.1465 & -1.1933 \\ -4.8614 & 9.8926 & -2.3027 & -7.5311 \\ 4.9984 & 2.3003 & 0.0116 & 7.3888 \\ -1.4566 & 8.3020 & -7.4043 & 8.8125 \end{bmatrix}$$

$$A_1^{c1} = \begin{bmatrix} -1.3890 & 0.6251 & 0.8055 & 0.0050 \\ 0.6251 & -1.5432 & 5.8555 & 0.0996 \\ 8.0546 & 5.8555 & -1.4325 & 0.0050 \\ 0.0050 & 9.9592 & 0.0555 & -1.5432 \end{bmatrix}$$

$$A_1^{c2} = \begin{bmatrix} -1.5380 & 0.6239 & 8.0389 & 0.0050 \\ 0.6239 & -1.5380 & 5.8234 & 9.9109 \\ 8.0393 & 5.8941 & -1.5380 & 0.0045 \\ 0.0023 & 9.9109 & 0.0032 & -1.5380 \end{bmatrix}$$

$$A_2^{c1} = \begin{bmatrix} -9.5788 & 3.6859 & -7.0714 & 2.8775 \\ 3.6886 & -64.3949 & 5.7497 & 5.8862 \\ -7.0717 & 5.7496 & -14.0720 & -0.0015 \\ 2.8776 & 5.8861 & -0.0015 & -14.1340 \end{bmatrix}$$

$$A_2^{c2} = \begin{bmatrix} -5.0459 & 0.0016 & -1.8510 & 7.1262 \\ 0.0016 & -25.02722 & 1.9712 & 2.0820 \\ -1.8509 & 1.9712 & -55.4083 & 0.0028 \\ 7.1260 & 2.0820 & 0.0028 & -55.2788 \end{bmatrix}$$

$$C_1^c = \begin{bmatrix} 4.3217 & 5.0016 & -3.5669 & 3.3349 \end{bmatrix}$$

$$C_2^c = \begin{bmatrix} 3.9020 & 4.6024 & -3.7504 & 3.8504 \end{bmatrix}$$

$$L_1^c = \begin{bmatrix} 4.0973 & -4.1144 & -9.8664 \\ 4.4914 & -8.3367 & -6.6930 \\ -3.1851 & -8.3367 & 4.7437 \\ 3.1346 & -6.3353 & 1.5748 \end{bmatrix}$$

$$L_2^c = \begin{bmatrix} 2.1998 & -3.1449 & -8.2809 \\ 4.1285 & -5.9593 & -1.2711 \\ -3.3094 & -4.7967 & 1.1038 \\ 7.4055 & -9.6537 & 1.0948 \end{bmatrix}$$

So next, for the simulation, we choose the initial states $x(0) = [0, 1, 0, 1]^T$ and $x_c(0) = [0, 0, 0, 1]^T$, and then set the external simple disturbance to $\omega(t) = 0.08sin(2\pi t)$. And by combining with Carsim-Simulink, we get from sensor to controller

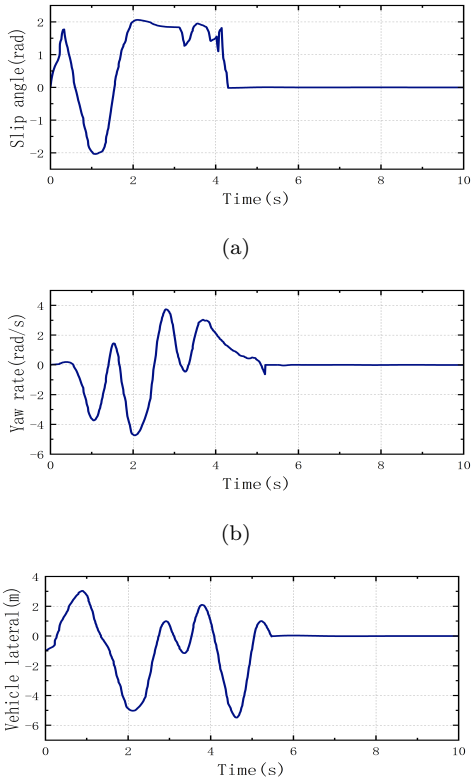

Figure 4: The three figures are lateral offset, yaw angle and yaw rate respectively, which are the measured values of the vehicle's state response in the sensor in the Carsim.

Select the output in the Carsim as Sliding angle beta vehicle, Yaw rate (body-fixed) vehicle and Lateral offset, objec. Then select the simple corner in the 3D road, and the final three measurements are Fig. 4.As the road is irregular and the actual situation of the car, so the overall appearance is not regular. That's exactly what's needed.In Fig. 5, when the mixed attack is considered, the non-response in the DoS attack in C-A is shown. At the same time, after experiencing deception attacks and replay attacks, the control input $u(t)$.After AETM in S-C, the release moment and release interval are shown in Fig. 6. It

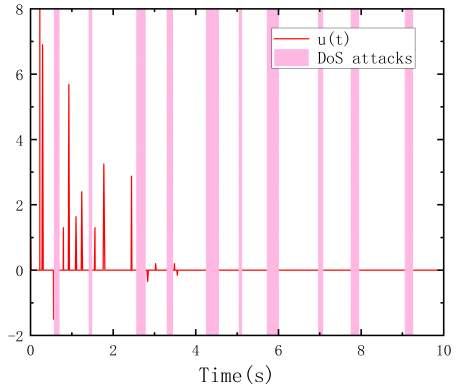

Figure 5: Control input $u(t)$ to the vehicle under hybrid attack.

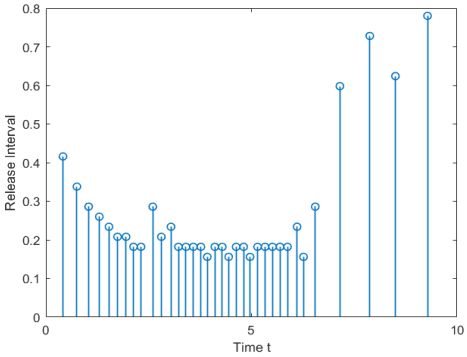

Figure 6: Release instants and release intervals of AETM in S-C channel.

can be seen that the data is greatly reduced through quantization and then event triggering, which greatly reduces the burden of the channel. It makes the transmission more efficient.

And then, the controller goes into the channel of the actuator, after quantization by the quantizers, and then the trigger coefficient σ_c is set as 0.05. After event triggering, the channel burden is further reduced. After hybrid attack.

The state response of the output feedback controller is shown as Fig. 7. It can be seen that it fluctuates greatly in the early stage and gradually fluctuates around 0 point later.After passing through the S-C channel, the input to the controller as shown in Fig. 8, transmission is blocked in the event of attacks. In the C-A channel, Fig. 9 represents

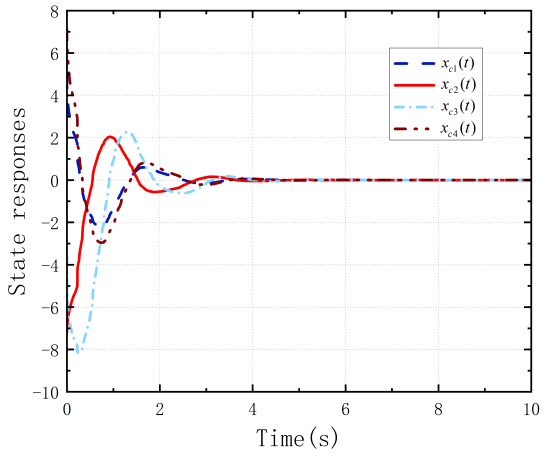

Figure 7: State responses $x_{c1} - x_{c4}$ of the controller.

the release moment and release interval, and the number of triggers is 27.

Table 2: Number of transmissions under different ET

Method	S-C	C-A	S-C transmission	C-A transmission
AETS $\sigma_s = 0.5, \sigma_c = 0.05$	35	27	17.5%	13.5%
ETS $\sigma_s = \sigma_c = 0.5$	30	17	15%	8.5%
ETS $\sigma_s = \sigma_c = 0.05$	53	46	26.5%	23%

Table 3: Transimissions rate of different sample time with $\sigma_s = \sigma_c = 0.5$

Sample time	0.01	0.05	0.1	0.2	0.3
Total times	62	47	38	30	27
Transimiision rate	31%	23.5%	19%	15%	13.5%

With the same sampling time, it can be seen from Table 2 that AETS has more data transfer than ETS with a transfer rate of 17.5% and 13.5%. Compared with $\sigma_s = \sigma = 0.05$ in ET, the transmission rate is lower and the channel is more saved.Therefore, ATETS has higher efficiency.As shown in Table 3, under the same trigger coefficient, the longer the sampling time, the lower the transmission rate. Thus, in the simulation, the system still follows stability even under hybrid attack.The system uses quantizers and AETS to make the channel transmission more efficient and more stable under hybrid attack.

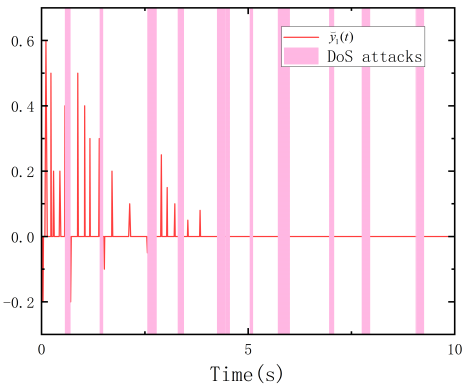

(a)

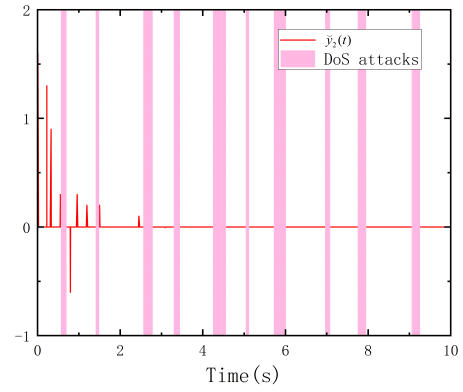

(b)

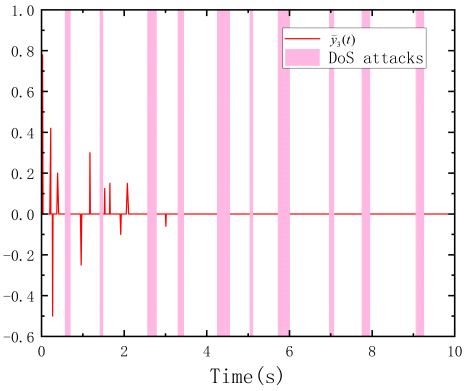

(c)

Figure 8: Controller input $y_1 - y_3$ after quantizers, event triggers, and hybrid attacks.

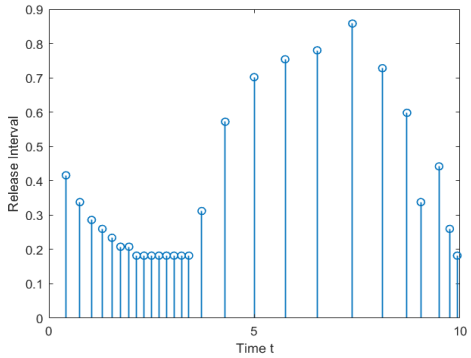

Figure 9: Release instants and release intervals of AETM in C-A channel.

5. Conclusion

In this paper, the lateral Angle control problem of vehicle in nonlinear dynamic system is studied. In the mixed case of three attacks, there will be strong instability, using the new output feedback controller, as well as two bandwidth saving schemes, make the dual channel stable, make the whole system stable. One is Resilient Asynchronous Event-Triggered Schemes, and the other is a pair of quantizers. Using the actual situation of the vehicle can be collected to achieve vehicle control. The simulation results show that accurate road tracking and vehicle stability can be achieved in the case of external interference and hybrid network attack. In combination with the study in this paper, further studies can be made on the control of more complex road conditions such as longitudinal and transverse vehicle, steep road and slope. And since the point of attack is the channel, the actual attack is more uncertain, and also a subsequent direction.

References

[1] N. Mansouri, A. Boukabou, et al., "Dynamic output feedback robust h control of networked control systems with time-varying delays via ts fuzzy models," Journal of the Franklin Institute, vol. 359, no. 15, pp. 8127–8154, 2022.

[2] W. Ma, X.-C. Jia, F. Yang, and X. Chi, "Fuzzy dynamic output feedback control for nonlinear networked multirate sampled-data systems: An integral inequality method," Fuzzy Sets and Systems, 2022.

[3] Z. Ye, D. Zhang, J. Cheng, and Z.-G. Wu, "Event-triggering and quantized sliding mode control of umv systems under dos attack," IEEE Transactions on Vehicular Technology, 2022.

[4] Y. Gao, J. Liu, Z. Wang, and L. Wu, "Interval type-2 fnn-based quantized tracking control for hypersonic flight vehicles with prescribed performance," IEEE transactions on systems, man, and cybernetics: systems, vol. 51, no. 3, pp. 1981–1993, 2019.

[5] J. Manigel and W. Leonhard, "Vehicle control by computer vision," IEEE Transactions on industrial electronics, vol. 39, no. 3, pp. 181–188, 1992.

[6] C. Zhang, H.-K. Lam, J. Qiu, P. Qi, and Q. Chen, "Fuzzy-model based output feedback steering control in autonomous driving subject to actuator constraints," IEEE Transactions on Fuzzy Systems, vol. 29, no. 3, pp. 457–470, 2019.

[7] T. Tiwari, S. Agarwal, and A. Etar, "Controller design for autonomous vehicle," in 2021 International Conference on Advances in Electrical, Computing, Communication and Sustainable Technologies (ICAECT), pp. 1–5, IEEE, 2021.

[8] L. Alonso, J. Perez-Oria, B. M. Al-Hadithi, and A. Jimenez, "Self-tuning pid controller for autonomous car tracking in urban traffic," in 2013 17th International Conference on System Theory, Control and Computing (ICSTCC), pp. 15–20, IEEE, 2013.

[9] S.-H. Lee and C. C. Chung, "Autonomous-driving vehicle control with composite velocity profile planning," IEEE Transactions on Control Systems Technology, vol. 29, no. 5, pp. 2079–2091, 2020.

[10] M. Brown, J. Funke, S. Erlien, and J. C. Gerdes, "Safe driving envelopes for path tracking in autonomous vehicles," Control Engineering Practice, vol. 61, pp. 307–316, 2017.

[11] C. Zhang, H.-K. Lam, J. Qiu, P. Qi, and Q. Chen, "Fuzzy-model based output feedback steering control in autonomous driving subject to actuator constraints," IEEE Transactions on Fuzzy Systems, vol. 29, no. 3, pp. 457–470, 2019.

[12] C. Zhang, J. Hu, J. Qiu, W. Yang, H. Sun, and Q. Chen, "A novel fuzzy observer-based steering control approach for path tracking in autonomous vehicles," IEEE Transactions on Fuzzy Systems, vol. 27, no. 2, pp. 278–290, 2018.

[13] Z. Lian, P. Shi, and C. C. Lim, "Dynamic hybrid-triggered-based fuzzy control for nonlinear networks under multiple cyberattacks," IEEE Transactions on Fuzzy Systems, vol. 30, no. 9, pp. 3940–3951, 2021.

[14] S.-G. Cao, N. W. Rees, and G. Feng, "Analysis and design of fuzzy control systems using dynamic fuzzy global models," Fuzzy sets and systems, vol. 75, no. 1, pp. 47–62, 1995.

[15] S.-G. Cao, N. W. Rees, and G. Feng, "Analysis and design for a class of complex control systems part ii: Fuzzy controller design," Automatica, vol. 33, no. 6, pp. 1029–1039, 1997.

[16] S. Zhang, J. He, Y. Yang, and T. Yan, "An outlier-resistant approach to observer-based security control for interval type-2 t-s fuzzy systems subject to deception attacks," IET Control Theory & Applications, 2022.

[17] G. Ran, C. Li, R. Sakthivel, C. Han, B. Wang, and J. Liu, "Adaptive event-triggered asynchronous control for interval type-2 fuzzy markov jump systems with cyberattacks," IEEE Transactions on Control of Network Systems, vol. 9, no. 1, pp. 88–99, 2022.

[18] K. Naik and C. P. Gupta, "Performance comparison of type-1 and type-2 fuzzy logic systems," in 2017 4th International Conference on Signal Processing, Computing and Control (ISPCC), pp. 72–76, IEEE, 2017.

[19] M.-Y. Lee and B.-S. Chen, "Robust h network observer-based attack tolerant path tracking control of autonomous ground vehicle," IEEE Access, 2022.

[20] Y. Gao, J. Liu, Z. Wang, and L. Wu, "Interval type-2 fnn-based quantized tracking control for hypersonic flight vehicles with prescribed performance," IEEE transactions on systems, man, and cybernetics: systems, vol. 51, no. 3, pp. 1981–1993, 2019.

[21] J. Wang, X. Liu, J. Xia, H. Shen, and J. H. Park, "Quantized inter val type-2 fuzzy control for persistent dwell-time switched nonlinear systems with singular perturbations," IEEE transactions on cybernetics, 2021

[22] S. Liu, Z. Wang, L. Wang, and G. Wei, "H pinning control of complex dynamical networks under dynamic quantization effects: A coupled backward riccati equation approach," IEEE Transactions on Cybernetics, 2020.

[23] X. Cai, K. Shi, K. She, S. Zhong, and Y. Tang, "Quantized sampled data control tactic for ts fuzzy ncs under stochastic cyber-attacks and its application to truck-trailer system," IEEE Transactions on Vehicular Technology, 2022.

[24] C. Gong, G. Zhu, and P. Shi, "Adaptive event-triggered and double quantized consensus of leader–follower multiagent systems with semi markovian jump parameters," IEEE Transactions on Systems, Man, and Cybernetics: Systems, vol. 51, no. 9, pp. 5867–5879, 2019.

[25] D. Yue, E. Tian, and Q.-L. Han, "A delay system method for designing event-triggered controllers of networked control systems," IEEE Transactions on automatic control, vol. 58, no. 2, pp. 475–481, 2012.

[26] Y. Pan, Y. Wu, and H.-K. Lam, "Security-based fuzzy control for nonlinear networked control systems with dos attacks via a resilient event-triggered scheme," IEEE Transactions on Fuzzy Systems, 2022.

[27] S. Hu, D. Yue, C. Dou, X. Xie, Y. Ma, and L. Ding, "Attack resilient event-triggered fuzzy interval type-2 filter design for networked nonlinear systems under sporadic denial-of-service jamming attacks," IEEE Transactions on Fuzzy Systems, vol. 30, no. 1, pp. 190–204, 2020.

[28] X. Li and D. Ye, "Asynchronous event-triggered control for networked interval type-2 fuzzy systems against dos attacks," IEEE Transactions on Fuzzy Systems, vol. 29, no. 2, pp. 262–274, 2020.

[29] Z. Lian, P. Shi, C.-C. Lim, and X. Yuan, "Fuzzy-model-based lateral control for networked autonomous vehicle systems under hybrid cyber attacks," IEEE Transactions on Cybernetics, 2022.

[30] Y. Qi, S. Yuan, and B. Niu, "Asynchronous control for switched ts fuzzy systems subject to data injection attacks via adaptive event-triggering schemes," IEEE Transactions on Systems, Man, and Cybernetics: Systems, 2021.

[31] T. Yang and C. Lv, "A secure sensor fusion framework for connected and automated vehicles under sensor attacks," IEEE Internet of Things Journal, 2021.

[32] J. Yang, C. Zhou, Y.-C. Tian, and C. An, "A zoning-based secure control approach against actuator attacks in industrial cyber-physical systems," IEEE Transactions on Industrial Electronics, vol. 68, no. 3, pp. 2637–2647, 2020

[33] X. Song, R. Zhang, C. K. Ahn, and S. Song, "Adaptive event-triggered control of networked fuzzy pde systems under hybrid cyber-attacks," IEEE Transactions on Fuzzy Systems, 2022.

[34] J. Liu, Y. Wang, J. Cao, D. Yue, and X. Xie, "Secure adaptive-event triggered filter design with input constraint and hybrid cyber attack," IEEE Transactions on Cybernetics, vol. 51, no. 8, pp. 4000–4010, 2020.

[35] Z. Zhang and J. Dong, "Fault-tolerant containment control for it2 fuzzy networked multiagent systems against denial-of-service attacks and actuator faults," IEEE Transactions on Systems, Man, and Cybernetics: Systems, vol. 52, no. 4, pp. 2213–2224, 2021.

[36] Z. Lian, P. Shi, and C.-C. Lim, "Adaptive resilient control for cyber physical systems under cyberattack and input saturation," IEEE Transactions on Industrial Informatics, 2022.

[37] S. Dong, C. P. Chen, M. Fang, and Z.-G. Wu, "Dissipativity-based asynchronous fuzzy sliding mode control for t–s fuzzy hidden markov jump systems," IEEE Transactions on Cybernetics,

vol. 50, no. 9, pp. 4020–4030, 2019.

[38] G. Ran, C. Li, H.-K. Lam, D. Li, and C. Han, "Event-based dissipative control of interval type-2 fuzzy markov jump systems under sensor saturation and actuator nonlinearity," IEEE Transactions on Fuzzy Systems, 2020.

[39] C. Peng, M. Wu, X. Xie, and Y.-L. Wang, "Event-triggered predictive control for networked nonlinear systems with imperfect premise matching," IEEE Transactions on Fuzzy Systems, vol. 26, no. 5, pp. 2797– 2806, 2018.

[40] X. Cai, K. Shi, K. She, S. Zhong, and Y. Tang, "Quantized sampled data control tactic for ts fuzzy ncs under stochastic cyber-attacks and its application to truck-trailer system," IEEE Transactions on Vehicular Technology, 2022.

[41] J. Liu, Z.-G. Wu, D. Yue, and J. H. Park, "Stabilization of networked control systems with hybrid-driven mechanism and probabilistic cyber attacks," IEEE Transactions on Systems, Man, and Cybernetics: Systems, vol. 51, no. 2, pp. 943–953, 2019.

[42] K. Liu, E. Fridman, and K. H. Johansson, "Dynamic quantization of uncertain linear networked control systems," Automatica, vol. 59, pp. 248–255, 2015.